

---

# XIII

## Basics on the Observations of Gravitational Waves

Astroparticle Physics a.a. 2021/22

Maurizio Spurio

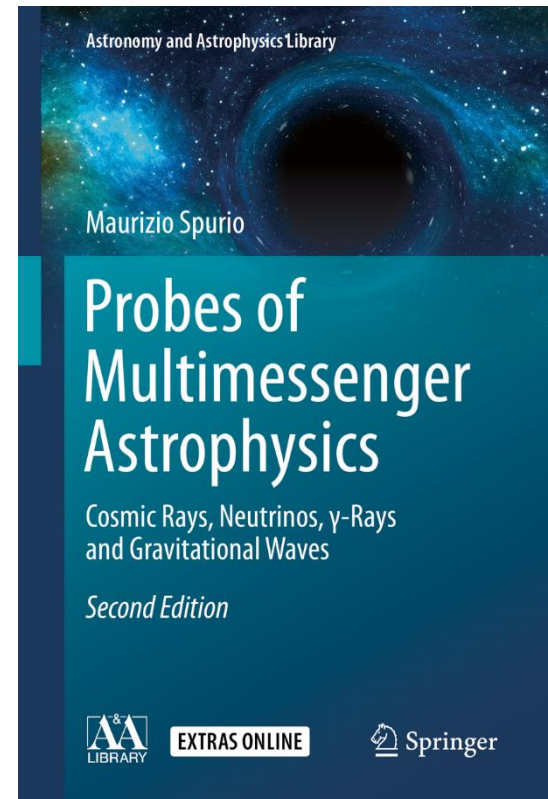
Università di Bologna e INFN

maurizio.spurio@unibo.it

# Content

---

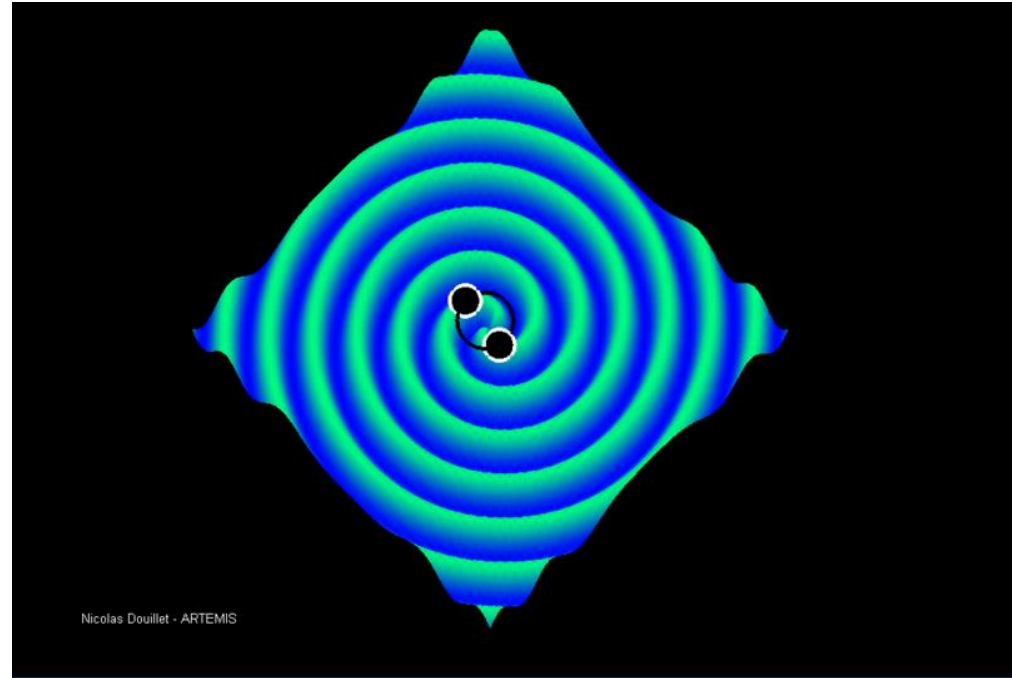
<b>13</b>	<b>Basics on the Observations of Gravitational Waves</b> .....
13.1	From Einstein Equation to Gravitational Waves .....
13.1.1	A Long Story Short .....
13.1.2	Summary of the Mathematical Background .....
13.2	Energy Carried by a Gravitational Wave .....
13.3	The Two-Body System .....
13.4	Ground-based Laser Interferometers .....
13.4.1	The Advanced LIGO Interferometers .....
13.4.2	Sensitivity of Ground-based Interferometers .....
13.5	GW150914 .....
13.5.1	Inspirational Stage .....
13.5.2	Coalescence Stage: Individual Masses .....
13.5.3	Luminosity Distance and Cosmological Effects .....
13.5.4	Total Emitted Energy .....
13.5.5	Ringdown Stage: Spin of the BHs .....
13.5.6	Source Localization in the Sky .....
13.6	Astrophysics of Stellar Black Holes after GW150914 .....
13.7	GW170817, GRB170817A and AT 2017gfo: One Event .....
13.7.1	GW170817 .....
13.7.2	GRB170817A .....
13.8	The Kilonova: Electromagnetic Follow-up of AT 2017gfo .....
13.9	Perspectives for Observational Cosmology after GW170817 .....
13.10	GW170817: The Axis Jet, the Afterglow and Neutrinos .....
13.11	Bursts of GWs from Stellar Gravitational Collapses .....
	References .....



# Gravitational Waves (GWs)

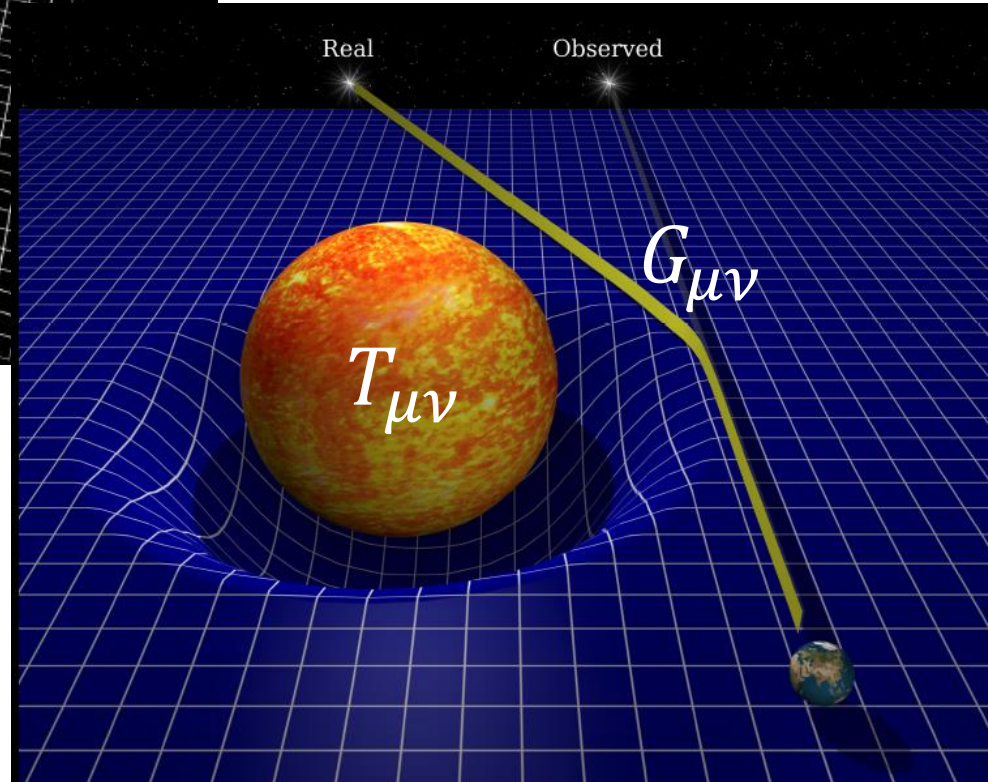
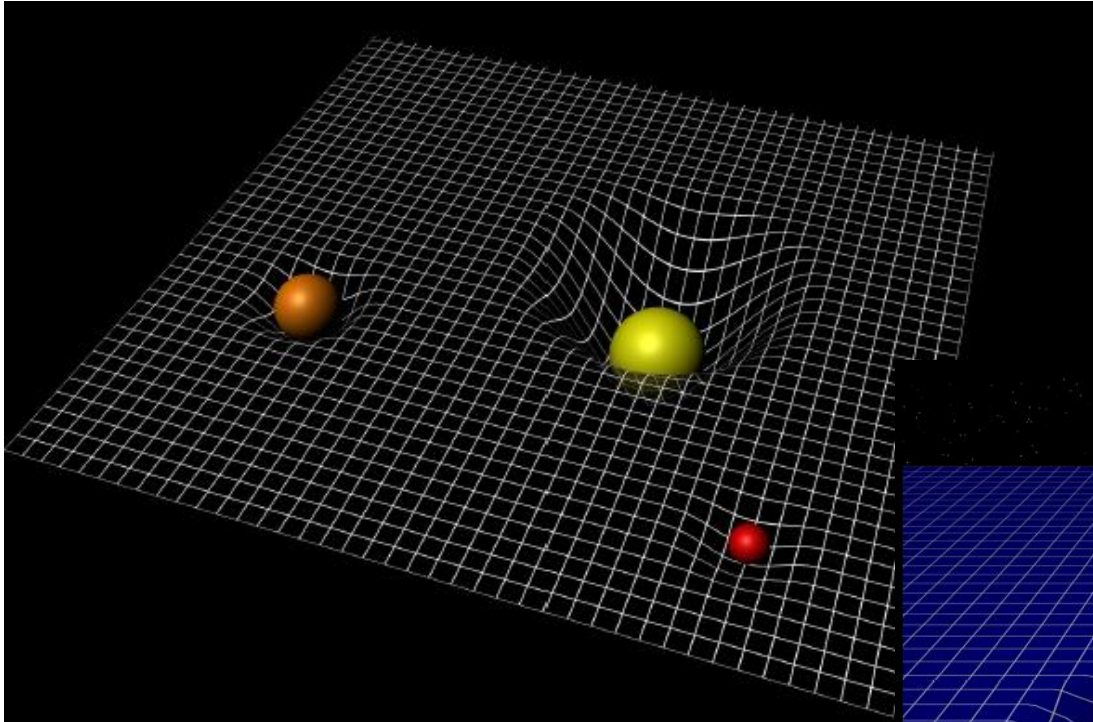
---

- GWs carry away large quantity of energy in systems involving movements of large masses
- Although the large amount of energy, GWs interact very weakly with matter and are difficult to detect.
- These properties make them ideal probes of some of the most interesting parts of the Universe, now that we have learned how to make sufficiently sensitive detectors.



- Unlike in most of electromagnetic astronomy, gravitational waves will be observed *coherently*, following the phase of the wave.
- This is possible because of their relatively low frequencies (below 10 kHz).
- **This makes detection strategies very different: instead of bolometric (energy) detection in hardware, gravitational wave detection will be in analyzing the phase.**
- The software for data analysis is of paramount importance

# General relativity





# From Einstein Equation to Gravitational Waves

---

- Gravitational waves (GW) are a natural consequence of Einstein's general theory of relativity, and their existence was predicted almost exactly 100 years ago.
- The starting point is the Einstein equations (**4x4 symmetric tensors**)

$$G_{\mu\nu} \equiv R_{\mu\nu} - \frac{1}{2}Rg_{\mu\nu} = \frac{8\pi G}{c^4}T_{\mu\nu} . \quad (13.3)$$



- Though simple in appearance, the Einstein equation is a nonlinear function of the metric and its first and second derivatives; this very compact geometrical statement disguises 10 coupled, nonlinear partial differential equations.
- In order to give a very simple mechanical analogy of (13.3), consider the potential energy connected with the spatial deformation of a spring:

$$kx = \nabla U . \quad (13.4)$$

- Thus, the equivalent of the spring's constant  $k$  in (13.3) is

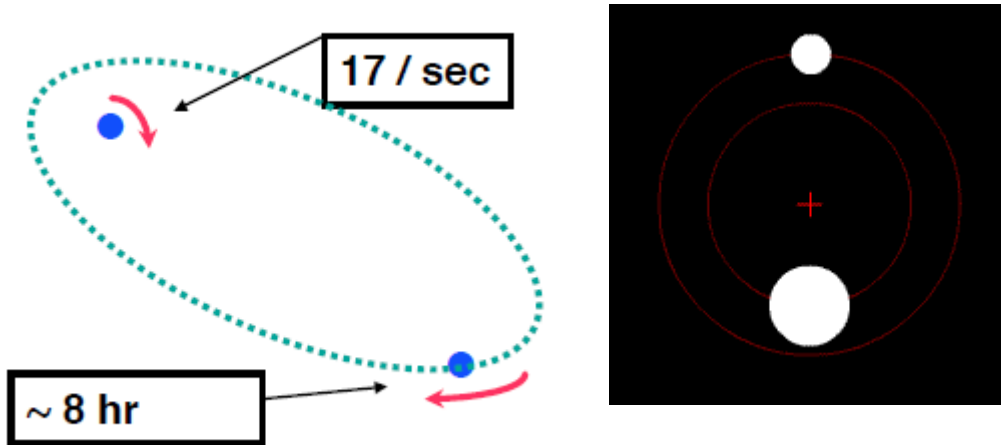
$$k \longrightarrow \frac{c^4}{8\pi G} = 5.6 \times 10^{45} \text{ kg m s}^{-2} . \quad (13.5)$$

# A Long Story Short

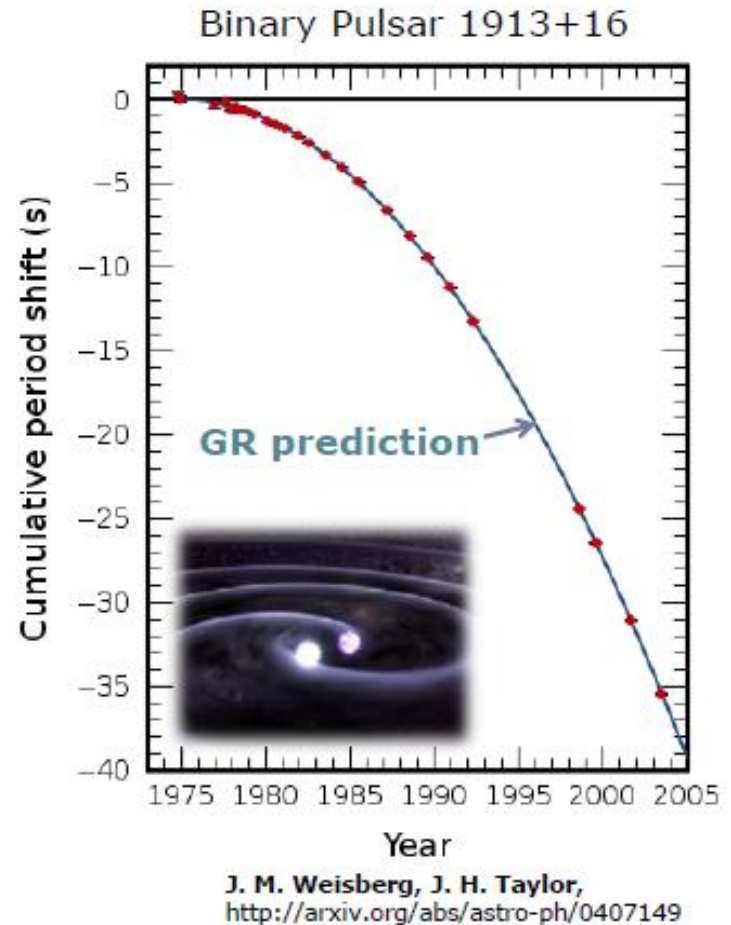
---

- The General Relativity (GR), published by Einstein in 1916 (during I Word War)
- Einstein derived three types of propagating solutions from the field equations; however, the nature of approximations led many (including Einstein himself) to doubt the result.
- In 1922, Eddington showed that two types of wave were artifacts. Eddington's joking sentence that GWs "**propagate at the speed of thought**".
- In 1936, Einstein and Nathan Rosen submitted a paper to the Physical Review Letter (PRL) with the title *Are there any gravitational waves?*
- The Einstein's epistolary documents show that the answer to the title was "NO".
- The editor sent the manuscript to be reviewed by an anonymous referee (in the usual peer review process), who questioned the conclusion of the paper.
- (Today, we know that the anonymous referee was Howard P. Robertson).
- Einstein angrily withdrew the manuscript, asserting that he would never publish in PRL
- Few weeks after Infeld (at that time, an assistant of Einstein) met Robertson at a conference, and Robertson convincing Infeld that the conclusion in his presentation (that contained in the Einstein-Rosen paper) was incorrect.
- Finally Infeld similarly convinced Einstein that the criticism was correct; the paper was rewritten with the same title, the opposite conclusion and published elsewhere.
- The question whether GWs carry energy (and are thus "physical" objects) or are instead a "gauge" effect **remained controversial up to the end of the 1950s.**

# GWs exist !



- 1974: Hulse-Taylor discover a pulsar in a binary system, with frequency of 17 Hz
- The pulsar orbits around a NS with an 8-hour orbital period
- In 30 years of observations, the orbital period has decreased by  $\sim 40$ s
- This is exactly what is expected for the loss of energy due to the GW emission (one of the few cases where the energy loss can be easily done)
- Nobel to Hulse and Taylor in 1993 for the indirect discovery of GW



# The Schwarzschild radius (Chap. 6)

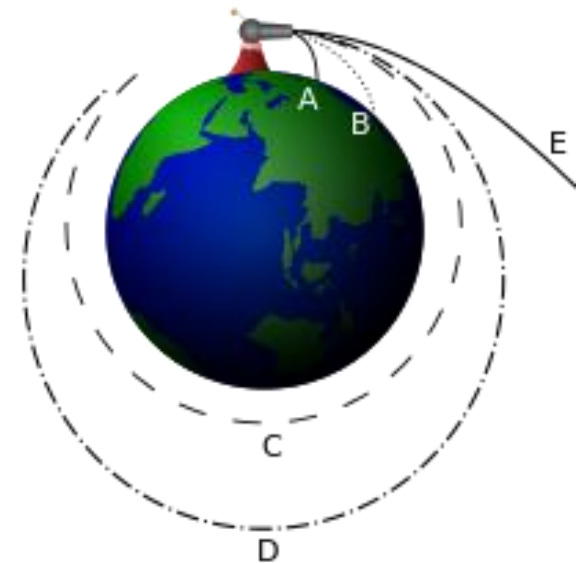
- A possible final state of the evolution of a massive star is a stellar black hole (or **stellar-mass black hole**). A black hole is a massive object exhibiting such strong gravitational effects that nothing (particles and electromagnetic radiation) can escape from inside its boundary, called the **event horizon**.
- In most cases, we can consider the event horizon equivalent to the **Schwarzschild radius** (This is correct for non-rotating massive objects that fit inside this radius).
- The escape velocity,  $v_{esc}$ , from a body of mass  $m$  at a distance  $r$  from the center is:

$$v_{esc} = \sqrt{2Gm/r}$$

- The Schwarzschild radius,  $R$ , is defined as the dimension of an object of mass  $m$  such that  $v_{esc} = c$ . Using the above relation, we obtain:

$$R = \frac{2Gm}{c^2} = 2.95 \left( \frac{m}{M_{\odot}} \right) \text{ km}, \quad (6.84)$$

- If the body is sufficiently dense and confined within  $R$ , the Schwarzschild radius represents its event horizon and its inner region behaves like a **black hole**.
- Particles and light can escape the black hole only if they remain outside the event horizon.





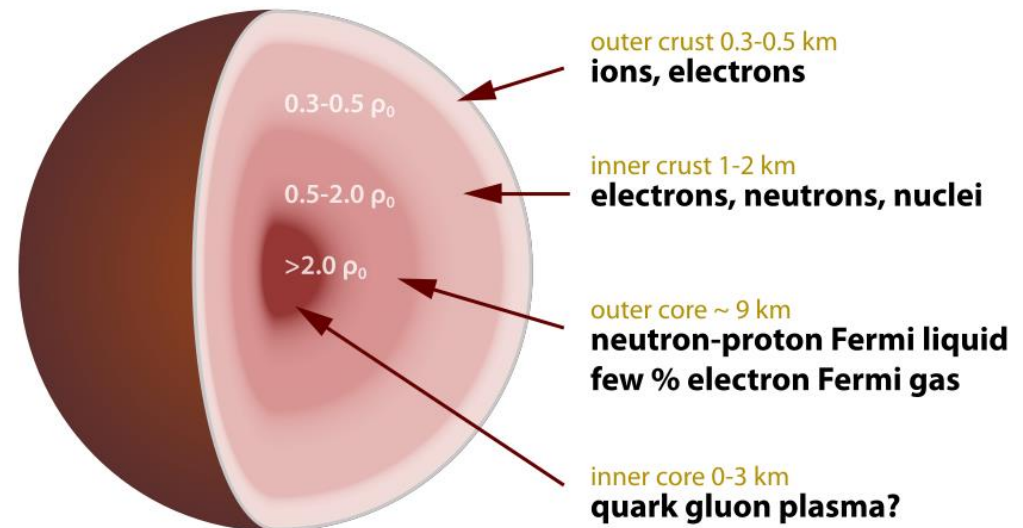
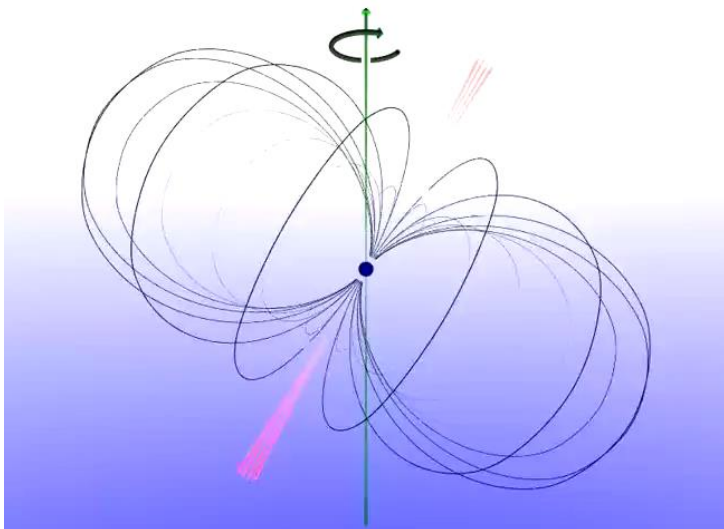
# Stellar Mass Black Holes (Chap. 6)

---

- By absorbing other stars and merging with other black holes, supermassive black holes of millions of solar masses may form.
- It is likely that supermassive BH exist in the centers of most galaxies.
- Although Eq. (6.84) is obtained from Newtonian considerations, the same conclusion emerges from general relativity. Furthermore, in classical general relativity, a particle that is inside the event horizon can never emerge outside.
- More generally, BHs are particular solutions to the Einstein field equations. It has been demonstrated (by the so-called **no-hair theorem**) that a stable black hole is completely described at any time by the following quantities:
  - **its mass-energy,  $M$ ;**
  - **its angular momentum, or spin,  $S$  (three components);**
  - **its total electric charge,  $Q$ .**
- In terms of these properties, four types of BHs can be defined:
  - Uncharged/Charged and non-rotating BHs (also called *Schwarzschild BH*)
  - Uncharged/Charged and rotating BHs (called *Kerr BHs*).
- A rotating BH is formed in the gravitational collapse of a massive spinning star;
- It can lose rotational energy through different mechanisms occurring just outside its event horizon. In that case, it gradually reduces to a Schwarzschild BH, the minimum configuration from which no further energy can be extracted.

# Neutron stars and pulsars (Chap. 6)

- A NS is an object with a defined mass,  $M_{\text{NS}} \sim 1.4M_{\text{sun}}$ , the Chandrasekhar mass
- Its density corresponds to the density of a nucleus,  $10^{14} \text{ g/cm}^3$ ,
- The radius of a neutron star is thus a few km (**exercise**)
- If the remnant star has a mass greater than the Chandrasekhar limit, it continues collapsing to form a **black hole**, Sect. 6.8.
- The details of their structure is unknown (the Equation of state, EoS)
- The maximum observed mass of neutron stars is  $\sim 2.0M_{\text{sun}}$



# From Einstein Equation to Gravitational Waves

- If we assume a weak gravitational field, the spacetime metric can be decomposed

$$g_{\mu\nu}(\mathbf{x}) = g_{\mu\nu}^{Cart} + h_{\mu\nu}(\mathbf{x}) . \quad (13.6)$$

- It exists a particular gauge condition under which (4) in vacuum

$$\left( -\frac{1}{c^2} \frac{\partial^2}{\partial t^2} + \nabla^2 \right) h_{\mu\nu}(\mathbf{x}) \equiv \square h_{\mu\nu}(\mathbf{x}) = 0 \quad (13.7)$$

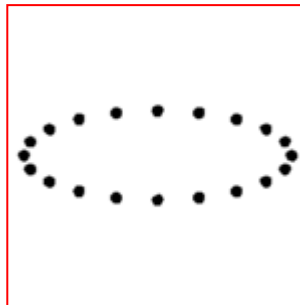
has familiar space-time dependence solutions, but describes a tensorperturbation

$$h_{\mu\nu}(\mathbf{x}) = h_{\mu\nu}^0 e^{[i(\mathbf{k}\cdot\mathbf{x} - \omega t)]} , \quad (13.8)$$

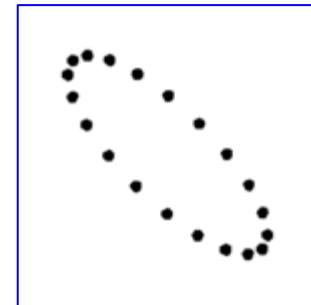
- The constant  $h^0$  is a symmetric 4x4 matrix and  $\omega = kc$ .

$$h_{\mu\nu}(\mathbf{x}) = \begin{pmatrix} 0 & 0 & 0 & 0 \\ 0 & h_+ & h_\times & 0 \\ 0 & h_\times & -h_+ & 0 \\ 0 & 0 & 0 & 0 \end{pmatrix} e^{[i(\mathbf{k}\cdot\mathbf{x} - \omega t)]} , \quad (13.9)$$

$h_+$

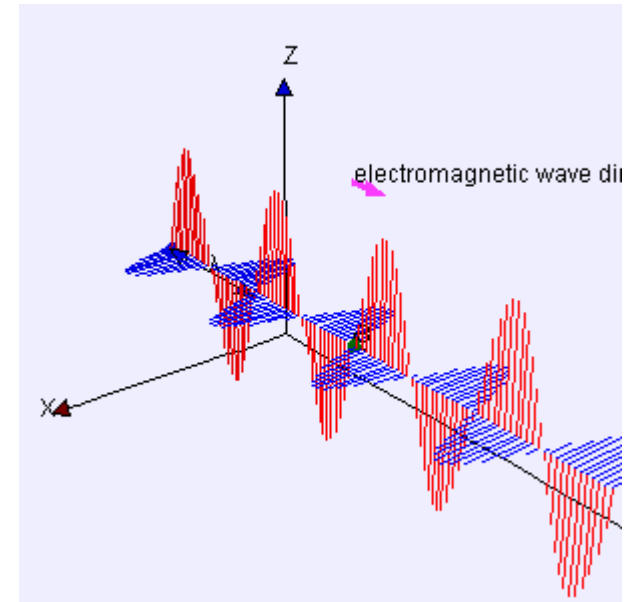


$h_\times$



# Analogies/differences between GW and EM (I)

1. The EM radiation is an incoherent superposition of light from many sources, in a region much larger than the radiation wavelengths; GWs come from sources with sizes  $R$  comparable to the wavelength  $\lambda$ . Hence the **signal reflects the coherent motion of extremely massive objects**.
2. Solutions of Maxwell's equations for a localized oscillating source of dimension  $R$  at a distance  $r$  in a homogeneous material are  $\mathbf{E}$  and  $\mathbf{B}$  fields that decay as  $1/r$  when  $r \gg R$ . These are the *radiating fields*; the condition  $r \gg R$  denotes the *far field*. Similarly, the strain  $h$  (see eq. 13.15)  $\propto 1/r$ .
3. The classical electromagnetic effect of a moving electric point charge in terms of a vector potential and a scalar potential is described by the **retarded Liénard–Wiechert potentials**. Retarded, because the effect on a position takes into account that the fields propagate at the speed of light  $c$ : 
$$t_{ret} = t - \frac{|\mathbf{r}-\mathbf{r}'|}{c}$$





# ONDA ELETTROMAGNETICA

- Potenziale  $\phi, \vec{A}$
- Campi: derivate dei potenziali  

$$\vec{E}, \vec{B} \rightarrow \frac{\partial}{\partial x_i} (\phi, \vec{A})$$

↳ coordinate spaziali
- Flusso di energia  

$$\vec{S} = \frac{\vec{E} \times \vec{B}}{\mu_0} \quad \left[ \frac{\text{Watt}}{\text{m}^2} \right]$$

dipende del "quadrato" dei campi

• Quanto vale il potenziale?  
 $\phi \propto \frac{\text{carica (sagente)}}{\text{distanza}}$

# ONDA GRAVITAZIONALE

- "potenziale"  $h$
- "Campo": deformazione della distribuzione due punti fissi nello spazio  
 campo  $\rightarrow h = \frac{dh}{dt}$  (solo tempo!)
- Flusso di energia  

$$\vec{F} \left[ \frac{\text{Watt}}{\text{m}^2} \right] = 0 \cdot |h|^2 \cdot \left( \frac{c^3}{G} \right) \rightarrow \text{dimensioni}$$

↳ quadrato del campo

costi difficili!!  $\frac{1}{32\pi}$

- Come stimare  $h$  per due masse in rotazione a distanza  $R$ ?

$\mu = \frac{m_1 m_2}{m_1 + m_2}$       $\mu = \frac{G m_1 m_2}{c^2 R}$       $\mu = \frac{G m_2}{c^2}$  = appioci S.

$$h \propto \left( \frac{G m_1}{c^2} \right) \left( \frac{G m_2}{c^2} \right) \cdot \frac{1}{R \cdot r}$$

$$h \propto \left( \frac{G M}{c^2 r} \right) \left( \frac{G \mu}{c^2 \cdot R} \right)$$

↳ potenziale  
↳ esterna "interno"

# Source terms

## Sviluppo in multipoli

ELETTROMAGNETISMO  $e = \int \rho \, dV$

ONDE GRAVITAZ  $m = \int \rho \, dV$

Effetto "ritardato"  
(potenziale di Liénard/Wiechert in EM)

$$\rho \rightarrow \rho\left(t - \frac{r}{c}\right)$$

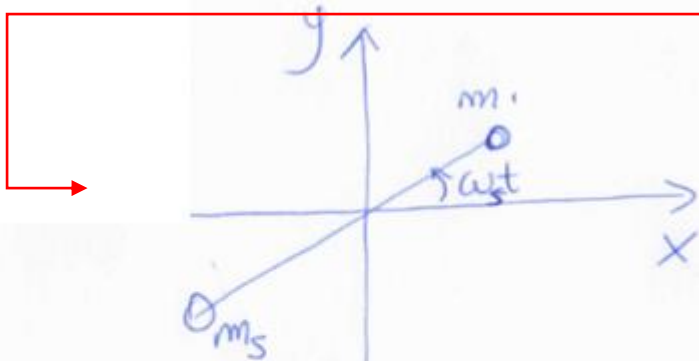
"MONOPOLO"  $\frac{d}{dt} \int \rho \, dV = 0$  (conservazione carica/massa)

"DIPOLO"  $\frac{d}{dt} \int \rho \cdot x \, dV \neq 0$  EM  
 $L = m \cdot v_{CM}$

le termini di dipolo non variano nel tempo  
Non produce onde gravitazionali  
(conservazione quantità di moto)

QUADRUPOLO  $\frac{d}{dt} \int \rho \cdot x \cdot y \, dV \neq 0$

$$\begin{aligned} \frac{d}{dt} \int \rho \cdot x \cdot y \, dV &= \frac{d}{dt} (h_0 \cdot \cos \omega_s t \cdot \sin \omega_s t) \\ &\cong \frac{d}{dt} (h_0 \cdot \sin 2\omega_s t) = \\ &\cong h_0 \cdot \omega_s \cdot \cos(\omega_g \cdot t) \end{aligned}$$



Due oggetti ruotanti attorno al proprio CM con frequenza  $\omega_s$  ("source")

$$\boxed{\omega_g = 2\omega_s}$$

La frequenza dell'onda GW è DOPPIA rispetto alla frequenza della sorgente

# Source term

---

- The inhomogeneous wave equation (in the presence of sources)

$$\square h_{\mu\nu}(\mathbf{x}) = \frac{16\pi G}{c^4} T_{\mu\nu} . \quad (13.10)$$

- It is analogous to the wave equation from a relativistic EM field

$$\square A^\mu(\mathbf{x}) = -\mu_0 J^\mu , \quad (13.11)$$

- the Green function formalism can be applied to derive a solution:

$$\mathbf{A}^\mu(t, \mathbf{x}) = \frac{\mu_0}{4\pi} \int d^3x' \frac{[\mathbf{J}(t', \mathbf{x}') ]_{ret}}{|\mathbf{x} - \mathbf{x}'|} \quad (13.12)$$

- Similarly, the solution for (11) produced by variations of the mass

$$h_{\mu\nu}(t, \mathbf{x}) = \frac{4G}{c^4} \int d^3x' \frac{[T_{\mu\nu}(t', \mathbf{x}') ]_{ret}}{|\mathbf{x} - \mathbf{x}'|} . \quad (13.13)$$

- That can be solved for a periodic system when

- 1)  $\lambda \gg R$ , i.e. the *long-wavelength approximation*, and
- 2)  $r \gg R$ , where  $r$  is the distance of the observer from the source (the *distant-source approximation*).

# The mass-quadrupole moment and energy flux

- Under these approximations, Eq. (14) connecting  $h$  and source reduces to

$$h_{\mu\nu}(t, \mathbf{x}) \simeq \frac{4G}{rc^4} \int d^3x' T_{\mu\nu}(t - r/c, \mathbf{x}'). \quad (13.14)$$

- This relation further simplifies if  $T$  is dominated by its rest-mass density, obtaining a relation for the spatial coordinates:

$$h_{ij} \simeq \frac{4G}{rc^4} \frac{d^2 Q_{ij}}{dt^2}, \quad (13.15)$$

- Where  $Q_{ij}$  is a 3x3 tensor of the mass quadrupole moment:

$$Q_{ij} = \int d^3x \left( x_i x_j - \frac{1}{3} r^2 \delta_{ij} \right) \rho_m(\mathbf{x}). \quad (13.16)$$

- If (16) holds, the GW carry an energy flux

$$\mathcal{F} = \frac{1}{32\pi} |\dot{h}|^2 \frac{c^3}{G}. \quad (13.18)$$

- That is the analogous of the Poynting vector for the EM wave:

$$\mathbf{S} = \frac{1}{\mu_0} \mathbf{E} \times \mathbf{B}.$$

**Exercise:** verify that that the quantity (13.18) has the same units of the Poynting vector

**Exercise:** verify that the (13.18) depends on  $1/r^2$



# Two-body system



- The quadrupole moment is defined as

$$Q_{ij} = \sum_{\alpha=1,2} m_{\alpha} \begin{pmatrix} \frac{2}{3}x_{\alpha}^2 - \frac{1}{3}y_{\alpha}^2 & x_{\alpha}y_{\alpha} & 0 \\ x_{\alpha}y_{\alpha} & \frac{2}{3}y_{\alpha}^2 - \frac{1}{3}x_{\alpha}^2 & 0 \\ 0 & 0 & -\frac{1}{3}r_{\alpha}^2 \end{pmatrix}. \quad (13.21)$$

- In the simple case of a binary system rotating at the frequency  $\nu_s$ :

$$Q_{ij}^{\alpha} = \frac{m_{\alpha}r_{\alpha}^2}{2} J_{ij}, \quad (13.22) \quad J_{ij} = \begin{pmatrix} \cos(2\omega_s t) + \frac{1}{3} & \sin(2\omega_s t) & 0 \\ \sin(2\omega_s t) & \frac{1}{3} - \cos(2\omega_s t) & 0 \\ 0 & 0 & -\frac{2}{3} \end{pmatrix}$$

- By summing up the contribution of the two masses

$$Q_{ij} = \sum_{\alpha=1,2} Q_{ij}^{\alpha} = \frac{1}{2} \mu R^2 J_{ij}, \quad (13.24) \quad \mu \equiv \frac{m_1 m_2}{m_1 + m_2} \quad (13.25)$$

- The second derivative of the quadrupole moment elements

$$\frac{d^2 Q}{dt^2} = \frac{1}{2} \mu R^2 \cdot (4\omega_s^2) \cdot \cos(2\omega_s t). \quad (13.27)$$

# The strain $h$ for a binary system

- For a 2-body system, the strain Eq. (16) is

$$h(t) \simeq \frac{4G}{rc^4} \cdot (2\mu R^2 \omega_s^2) \cdot \cos(2\omega_s t) = h_o \cos(\omega_{gw} t), \quad (13.28)$$

- Because the quadrupole moment is symmetric under  $180^\circ$  rotation about the orbital axis, **the radiation has a frequency,  $\omega_{gw}$ , twice that of the orbital frequency of the source,  $\omega_s$ .**

- The Kepler III law connect angular velocity and radius  $R$

$$\omega_s^2 = \frac{GM}{R^3} \quad \text{where } M = m_1 + m_2$$

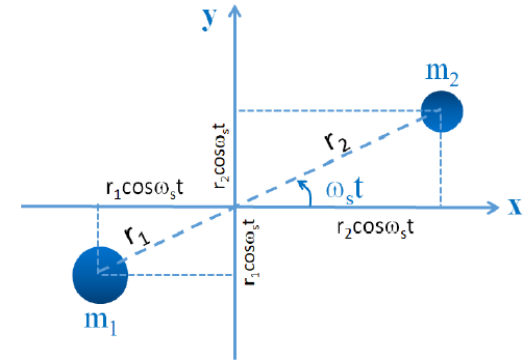
- Thus, the strain  $h_o$  in (28)  $h_o \simeq \frac{4G}{rc^4} \cdot (2\mu R^2) \frac{GM}{R^3}, \quad (13.30)$
- Or, in a form manifestly dimensionless:

$$h_o = 2 \left( \frac{2GM}{c^2 r} \right) \left( \frac{2G\mu}{c^2 R} \right) = 2 \frac{\mathcal{R}_{S_1} \cdot \mathcal{R}_{S_2}}{r \cdot R}. \quad (13.31)$$

# The flux $\mathcal{F}$ and luminosity $\mathcal{L}$

- We derived the energy flux , eq. (13.18) in units: (W/cm<sup>2</sup> s) of the GW.
- For the binary system, it can be simply written as:

$$\mathcal{F} = \frac{1}{32\pi} \frac{c^3}{G} h_o^2 \omega_{gw}^2, \quad (13.37)$$



**Important exercise** (see: arXiv:9710079 of B.F. Schutz)

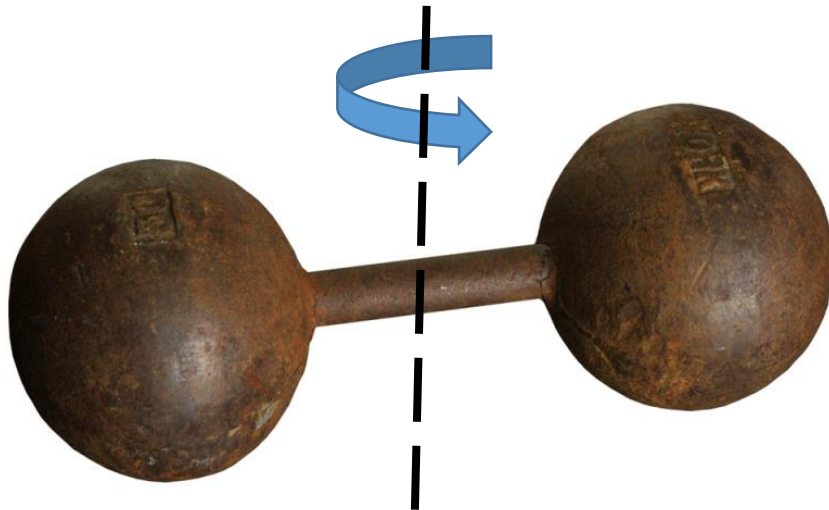
- Use the flux  $\mathcal{F}$  (13.37), and assume that is emitted isotopically over a sphere of radius  $r$ . Under this assumption, the luminosity at the source is given by:  $\mathcal{L} = 4\pi r^2 \mathcal{F}$
- Remember that  $\omega_{gw} = 2 \omega_s$ .
- Make use of the III Kepler law that correlate the distance  $R$  and  $\omega_s$ .
- Show that the luminosity  $\mathcal{L}$  can be simply written (without the factor 1/5) as (13.36):

$$\mathcal{L} = \frac{1}{5} \frac{G}{c^5} \cdot \left( \frac{1}{2} \mu R^2 \right)^2 \cdot (2\omega_s)^6 \cdot 2 = \frac{32}{5} \frac{G}{c^5} \cdot [\mu R^2 \omega_s^3]^2. \quad (13.36)$$

- (The factor 1/5 arises from the fact that the flux  $\mathcal{F}$  is not isotropic).

# Man-made Gravitational waves

- Differently from EM waves, it is almost impossible with current technology to produce and detect manmade GWs.



- **Exercise:** Consider a dumbbell consisting of two 1-ton compact masses with their centers separated by 2 m and spinning at 1 kHz (this is the limit for its stability). Determine the strain  $h_0$  to an observer 300 km away (in the far field region).
- **Answer:**  $h_0 \sim 10^{-38}$



# The strain and the effect on free masses (=observer)

- **Exercise:** Compute  $h_0$  for 2 neutron stars at  $R=100$  km and at 40 Mpc from the Earth

- **Answer:** 
$$h_0 = 2 \left( \frac{(4000 \text{ m})^2}{10^5 \times 1.2 \cdot 10^{24} \text{ m}^2} \right) \simeq 3 \times 10^{-22} . \quad (13.32)$$

- As a GW passes an observer, that observer (=free masses) will find space-time distorted by the effects of strain.
- **Distances  $L$  between objects increase and decrease rhythmically as the wave passes, with a maximum amplitude  $\Delta L$  such that**


$$\frac{\Delta L}{L} \cong h_0 .$$

- To get a feeling for this, the distance of the Earth from the Sun is changed by the distance of one atom during the passage of such a GW.
- With the quadrupole moment (13.22), the luminosity of the source from Eq. (13.19) is

# Analogies/differences between GW and EM (II)

---

... continues from 

4. Detectors of the electromagnetic radiation are sensible to the flux intensity (i.e. to the Poynting vector,  $\mathbf{S}$ ) that decreases as  $1/r^2$  : **work must be done on electric charges** of the detector. On the contrary, **GW detectors register waves coherently by following the phase of the wave and not just measuring its intensity**. The phase of the wave in the strain  $h$  that decreases as  $1/r$
5. The frequencies of detectable GWs are below the few kHz range; the graviton energies  $h\nu$  are very small, making detection of individual quanta extremely challenging (if not almost impossible)
6. Gravitational radiation suffers a very small absorption when passing through ordinary matter. As a result, GWs can carry to us information about violent processes occurred in very dense environments.
7. It is almost impossible with current technology to detect manmade GWs (see )

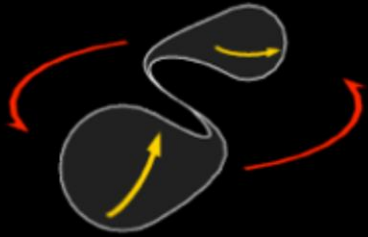
**Exercise:** A GW detector that measures the strain  $h_0$  improves the sensitivity (=minimum detectable signal) by a factor of 3. Before the improvement, the number of possible source visible in the Universe is  $N_0$ . Evaluate the number  $N_1$  of sources visible after the improvement. Compare the same situation for a telescope observing the EM radiation.

**Answer:** after improvement,  $N_1=3^3N_0$  for the GW observatory. It is  $N_1=3^{3/2}N_0$  for the EM telescopes.

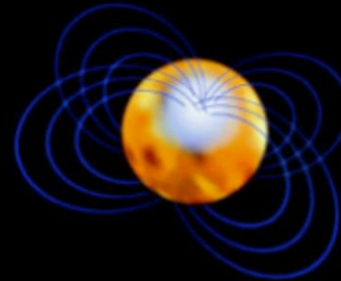
# Sources of Gravitational waves

---

- It is almost impossible to produce and detect manmade GWs.
- Different astrophysical sources of GW have been modeled



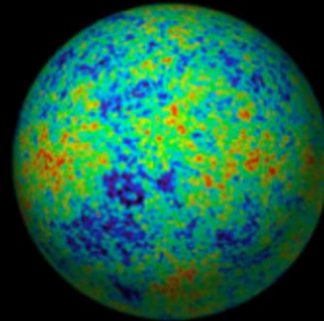
**Compact binary coalescence (CBC):**  
inspiral, merger and  
ringdown of black  
holes and neutron stars



**Continuous Sources:**  
spinning  
neutron stars

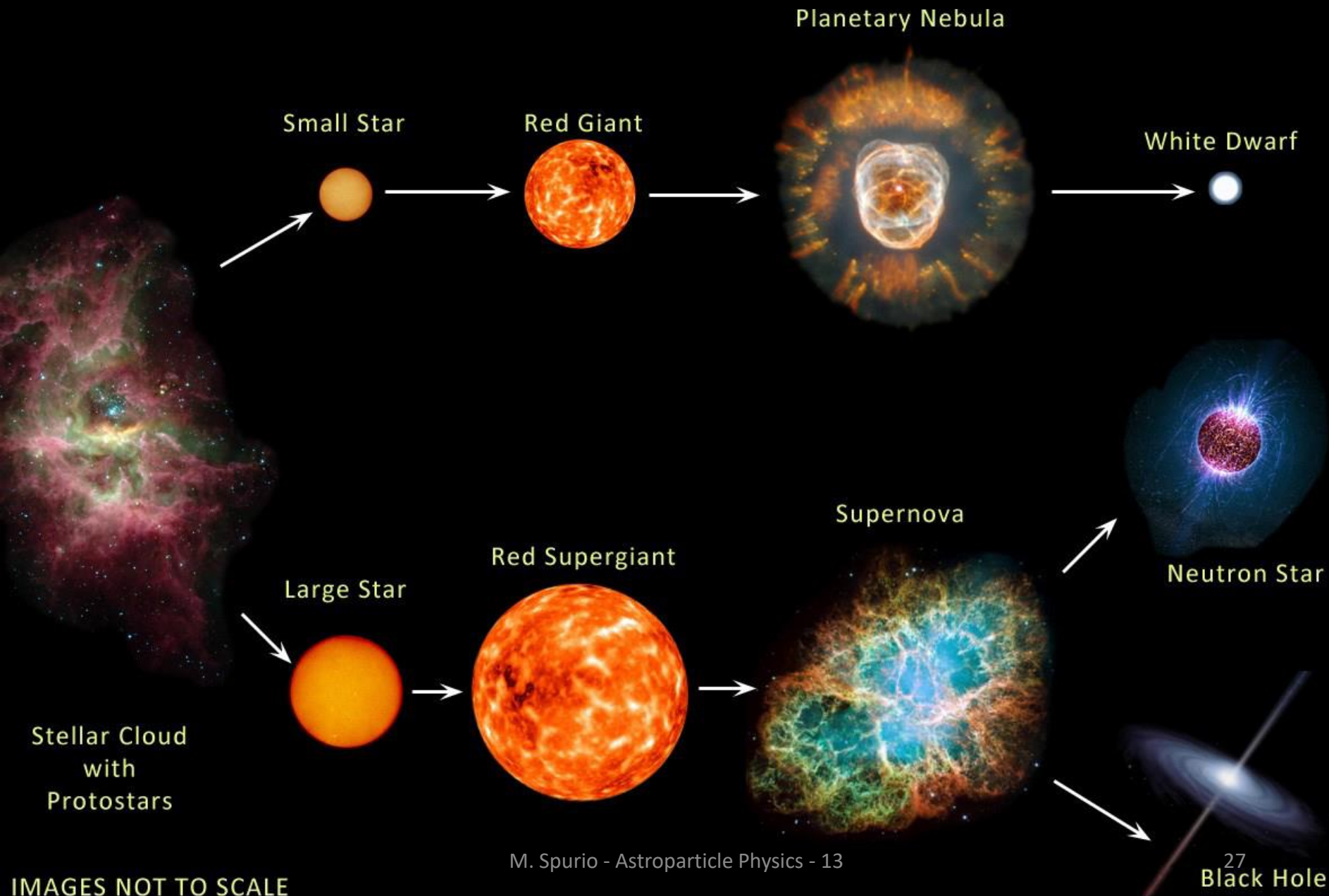


**Short bursts:**  
supernovae,  
unmodeled transient  
sources



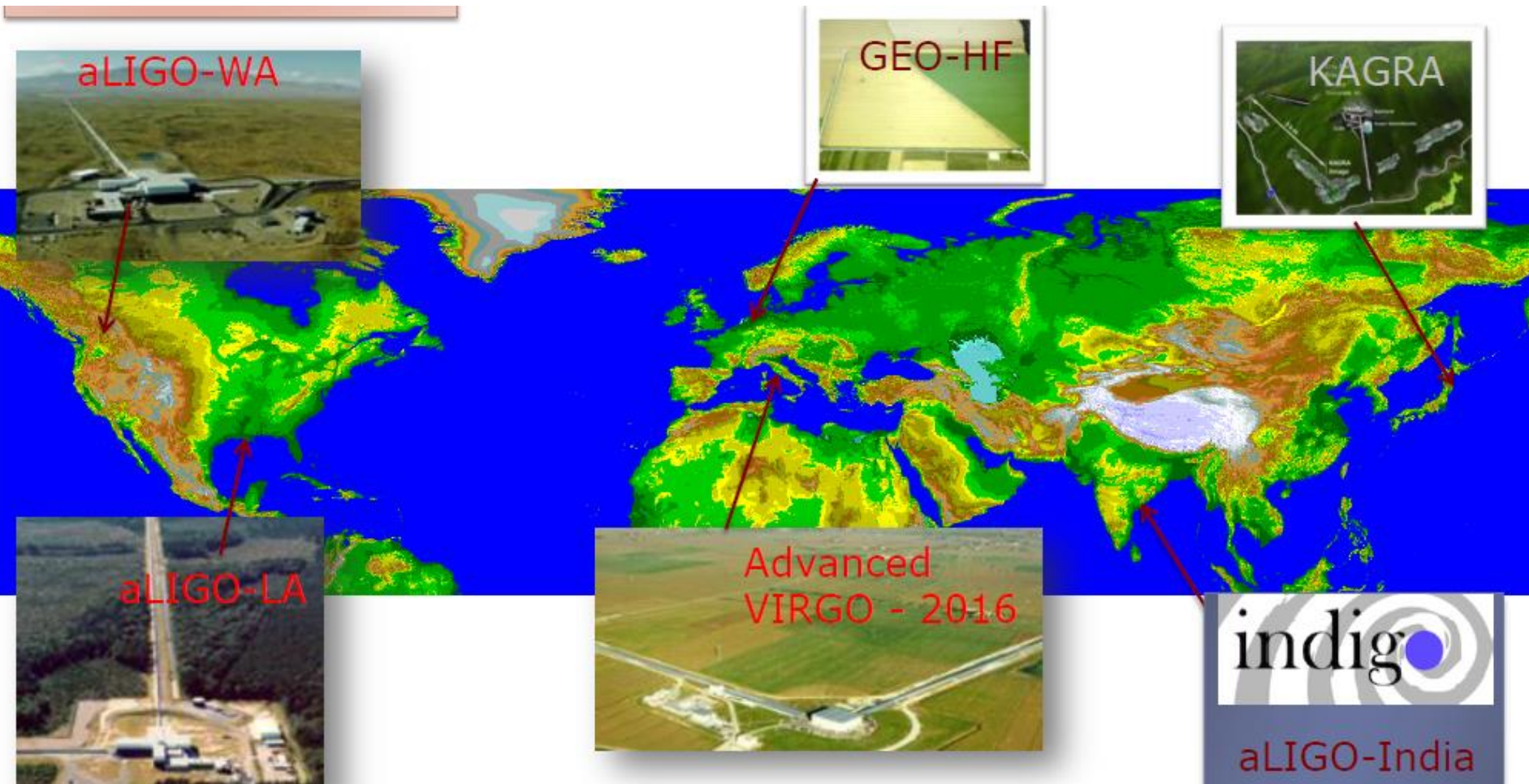
**Stochastic sources:**  
gravitational wave  
background from the  
big bang

# Evolution of stars






# Ground-based laser interferometers



# Detecting GWs, early tentative

- **Effect of GWs:** Squeeze and stretch the space in perpendicular directions: strain  $h = \Delta L/L$
- Detectors must be designed to achieve  $h < 10^{-22}$ , over the widest frequency range within 10-5000 Hz 
- The question **whether the waves carry energy remained controversial up to the end of the 1950s**. Finally, F. Pirani showed that GWs would exert tidal forces on intervening matter, producing a strain.
- This stimulated **experimental searches for GW with the work of Weber (1960)**, also motivated by incorrect predictions of  $h \sim 10^{-17}$  at  $1 \sim \text{kHz}$ .
- Weber built an aluminum bar 2 m in length and 0.5 m in diameter, with resonant mode of oscillation of 1,6 kHz. The bar was fitted with piezo-electric transducers to convert its motion into an electrical signal.
- In 1971, with the coincident use of two detectors (in Michigan and Illinois), Weber claimed detection of GWs from the direction of the galactic center.
- This led to the construction of many other bar detectors of comparable or better sensitivity, which never confirmed his claims.

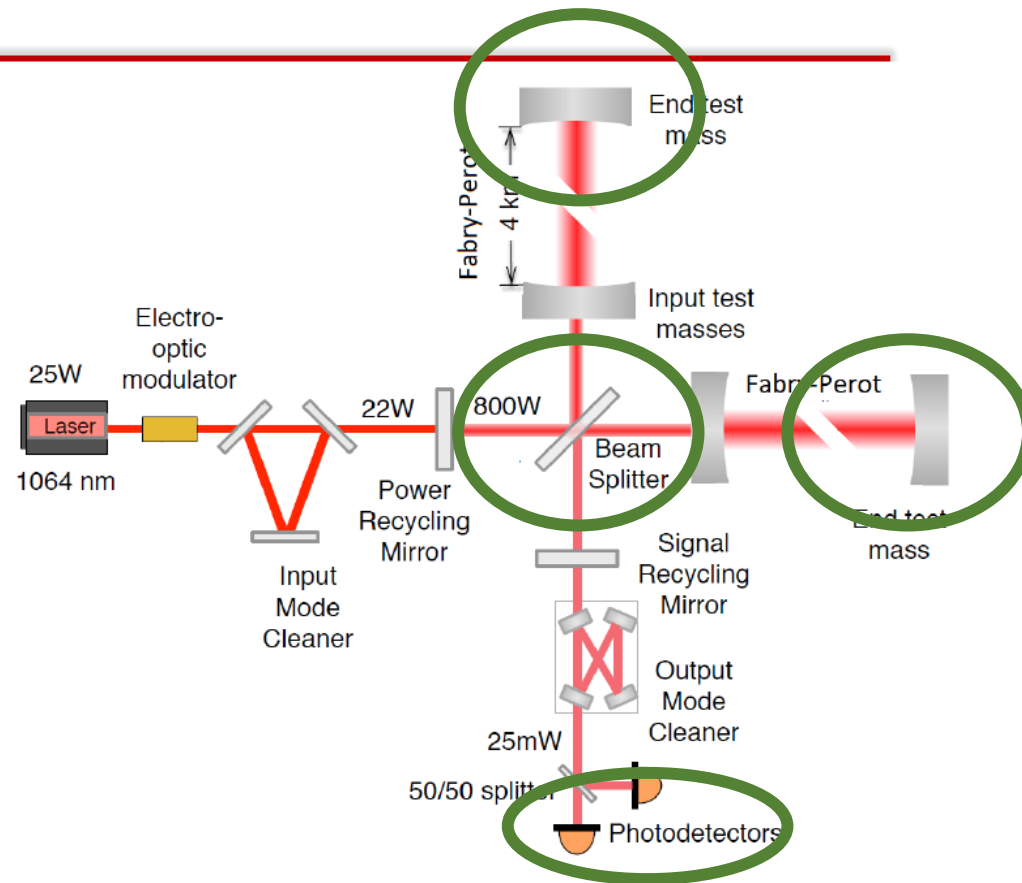
Joseph Weber c. 1965



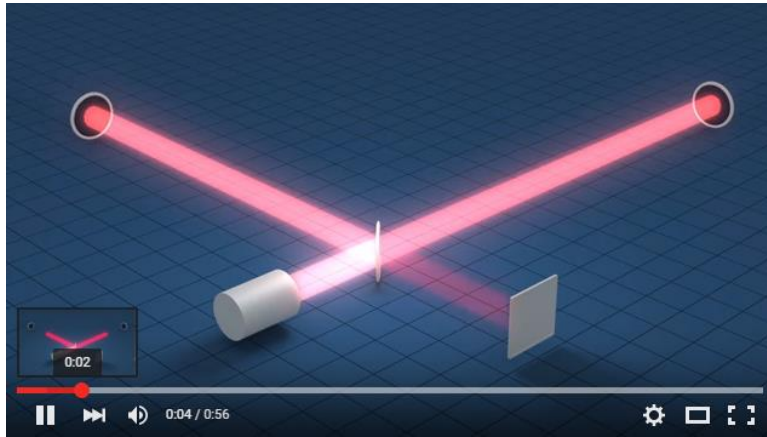


# Laser interferometers

- GW interferometers are arranged in Michelson configuration (L-shaped).
- They consist of a **laser**, a beam **splitter**, a series of **mirrors** and **photodetectors** that record the interference pattern.
- A beam splitter splits the laser beam into two identical beams, one at 90°.
- At the end of each arm, a mirror acting as a test mass reflects each beam back to the beam splitter, where the two beams merge back into a single beam.
- In 'merging', light waves interfere with each other before reaching a photodetector.
- GW interferometers are set up so that the interference is destructive.
- Any change in light intensity indicates that something (noise or signal) happened to change the distance  $L$  travelled by one or both laser beams.
- The interference pattern can be used to calculate  $\Delta L/L$ , i.e., the signal strain (13.33)



# The interferometers: LIGO (USA)



- LIGO consists of two widely separated (about 3,000 km) identical detector sites in the USA working as a single observatory: one in southeastern Washington State and the other in rural Livingston, Louisiana.



# VIRGO (Italy)

---

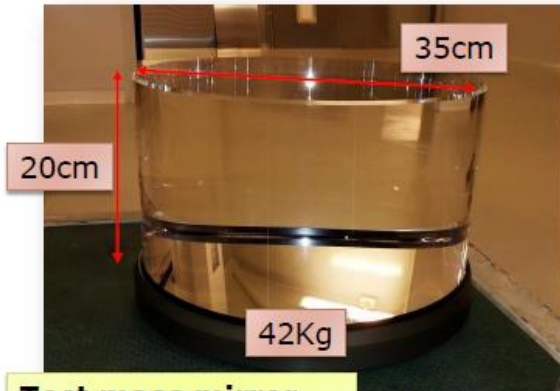
- Virgo is a 3 km interferometer located close to Pisa, Italy, funded by the European Gravitational Observatory (EGO), a collaboration between the Italian INFN and the French CNRS.



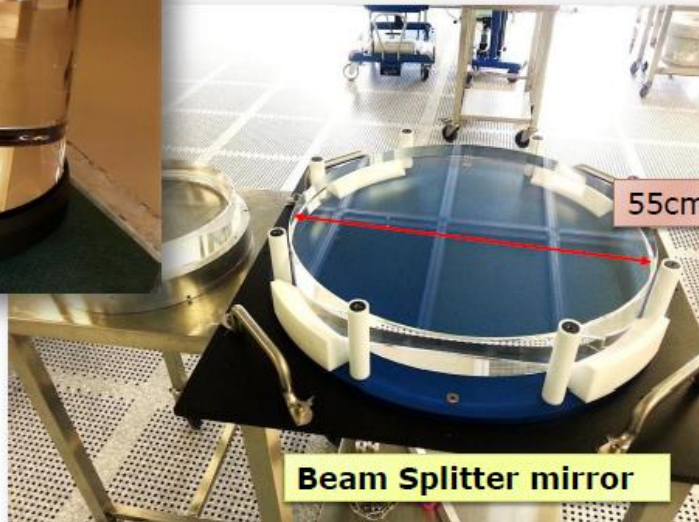


# Advanced LIGO/VIRGO runs O1-O2

- Initial LIGO and VIRGO took data between 2001 and 2010, without detecting GWs.
- The redesign, construction, preparation and installation of the Advanced LIGO (aLIGO) took 7 years, from 2008 to 2015, and those for the Advanced Virgo from 2010 to 2017.
- LIGO and Virgo Collaborations are separate organizations, **but they cooperate closely; they are referred to as LVC, and they collectively sign the research papers.**



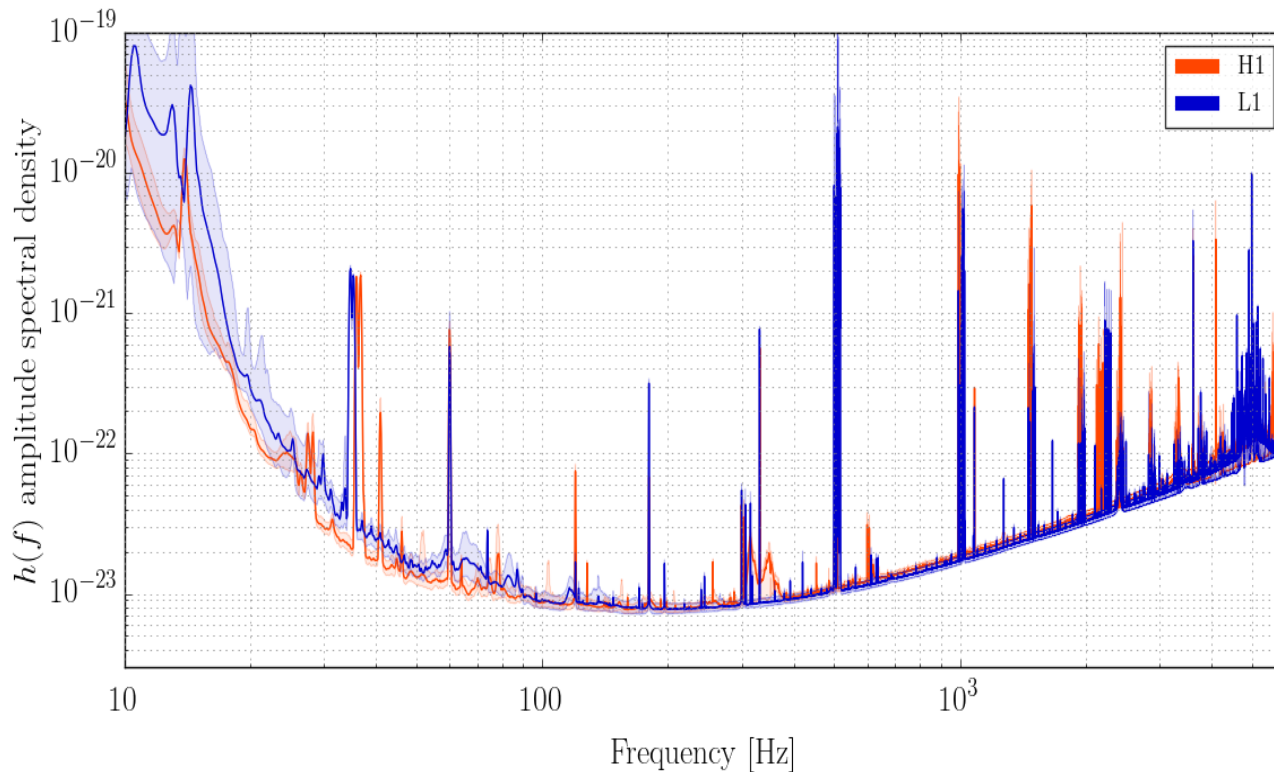
Test mass mirror



- September 2015: aLIGO began the era of GW astronomy with its first observation run (O1) and detections, collecting data until January 2016.
- The O2 run of aLIGO started on November 30, 2016. aVirgo joined the O2 run on August 1, 2017.
- O2 operations ended on August 25, 2017.
- O3 operations started on April 1<sup>st</sup>, 2019 end **March 27, 2020**

# Noise

- A genuine GW signal must be extracted from a large background due to noise sources. These noise sources can be divided into two categories:
  - **Displacement noises**, such as thermal noise, ground vibrations and gravity gradient noises. These dominate at the frequencies below 100 Hz.
  - **Sensing noises**, as shot noise and quantum effects. Associated with the conversion of displacement into a readout signal (dominates above 100 Hz).



*Noise at aLIGO at the time of GW150914. On the y axis there is an amplitude spectral density, expressed in terms of equivalent GW strain. Narrow-band features include calibration lines (33-38, 330, and 1,080 Hz), vibrational modes of suspension fibers (500 Hz and harmonics), and 60 Hz electric power grid harmonics*

The discovery

hole ringdown. Over 0.2 s, the signal increases in frequency and amplitude by about 8 cycles from 35 to 150 Hz, where the amplitude reaches a maximum. The most plausible explanation for this evolution is the inspiral of two orbiting masses,  $m_1$  and  $m_2$ , due to gravitational-wave emission. At the lower frequencies, such evolution is characterized by the chirp mass [11]

$$\mathcal{M} = \frac{(m_1 m_2)^{3/5}}{(m_1 + m_2)^{1/5}} = \frac{c^3}{G} \left[ \frac{5}{96} \pi^{-8/3} f^{-11/3} \dot{f} \right]^{3/5},$$

where  $f$  and  $\dot{f}$  are the observed frequency and its time derivative and  $G$  and  $c$  are the gravitational constant and speed of light. Estimating  $f$  and  $\dot{f}$  from the data in Fig. 1,

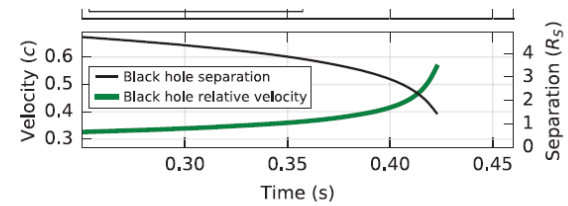


FIG. 2. *Top*: Estimated gravitational-wave strain amplitude from GW150914 projected onto H1. This shows the full bandwidth of the waveforms, without the filtering used for Fig. 1. The inset images show numerical relativity models of the black hole horizons as the black holes coalesce. *Bottom*: The Keplerian effective black hole separation in units of Schwarzschild radii ( $R_S = 2GM/c^2$ ) and the effective relative velocity given by the post-Newtonian parameter  $v/c = (GM\pi f/c^3)^{1/3}$  where  $f$  is the

Selected for a Viewpoint in *Physics*

PRL 116, 061102 (2016)

PHYSICAL REVIEW LETTERS

week ending  
12 FEBRUARY 2016

## Observation of Gravitational Waves from a Binary Black Hole Merger

B. P. Abbott *et al.*\*

(LIGO Scientific Collaboration and Virgo Collaboration)

(Received 21 January 2016; published 11 February 2016)

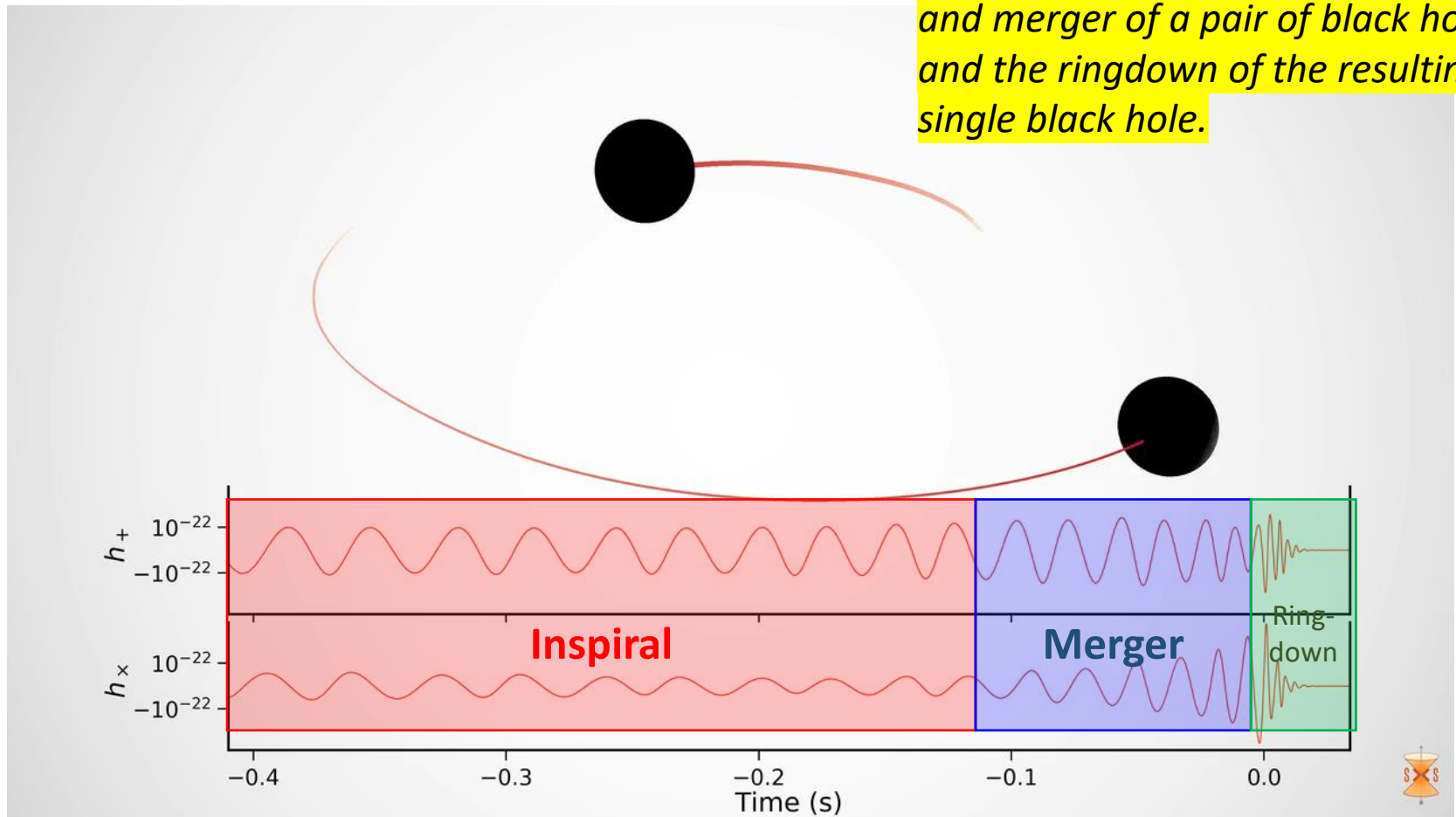
On September 14, 2015 at 09:50:45 UTC the two detectors of the Laser Interferometer Gravitational-Wave Observatory simultaneously observed a transient gravitational-wave signal. The signal sweeps upwards in frequency from 35 to 250 Hz with a peak gravitational-wave strain of  $1.0 \times 10^{-21}$ . It matches the waveform predicted by general relativity for the inspiral and merger of a pair of black holes and the ringdown of the resulting single black hole. The signal was observed with a matched-filter signal-to-noise ratio of 24 and a false alarm rate estimated to be less than 1 event per 203 000 years, equivalent to a significance greater than  $5.1\sigma$ . The source lies at a luminosity distance of  $410^{+160}_{-180}$  Mpc corresponding to a redshift  $z = 0.09^{+0.03}_{-0.04}$ . In the source frame, the initial black hole masses are  $36^{+5}_{-4} M_\odot$  and  $29^{+4}_{-4} M_\odot$ , and the final black hole mass is  $62^{+4}_{-4} M_\odot$ , with  $3.0^{+0.5}_{-0.5} M_\odot c^2$  radiated in gravitational waves. All uncertainties define 90% credible intervals. These observations demonstrate the existence of binary stellar-mass black hole systems. This is the first direct detection of gravitational waves and the first observation of a binary black hole merger.

DOI: 10.1103/PhysRevLett.116.061102



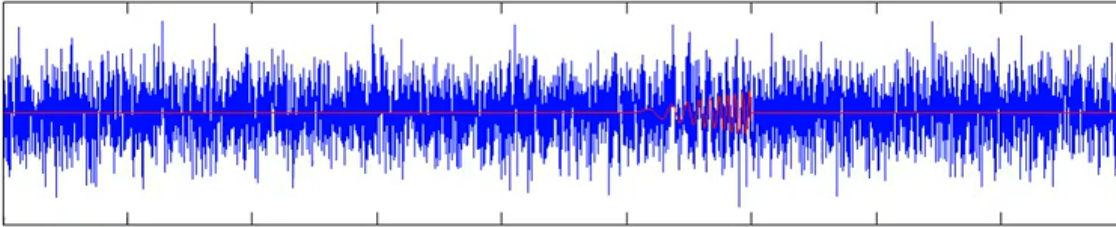
# The expected signal

*It matches the waveform predicted by general relativity for the inspiral and merger of a pair of black holes and the ringdown of the resulting single black hole.*

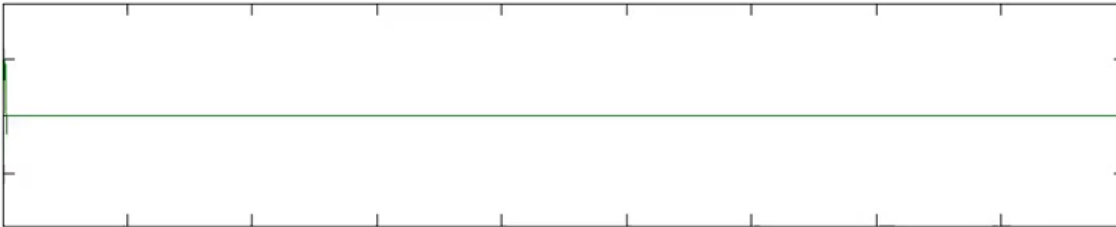


# Transient signal: the *matching* filter method

Data (signal buried in noise)



Signal Template



Cross-Correlation Result

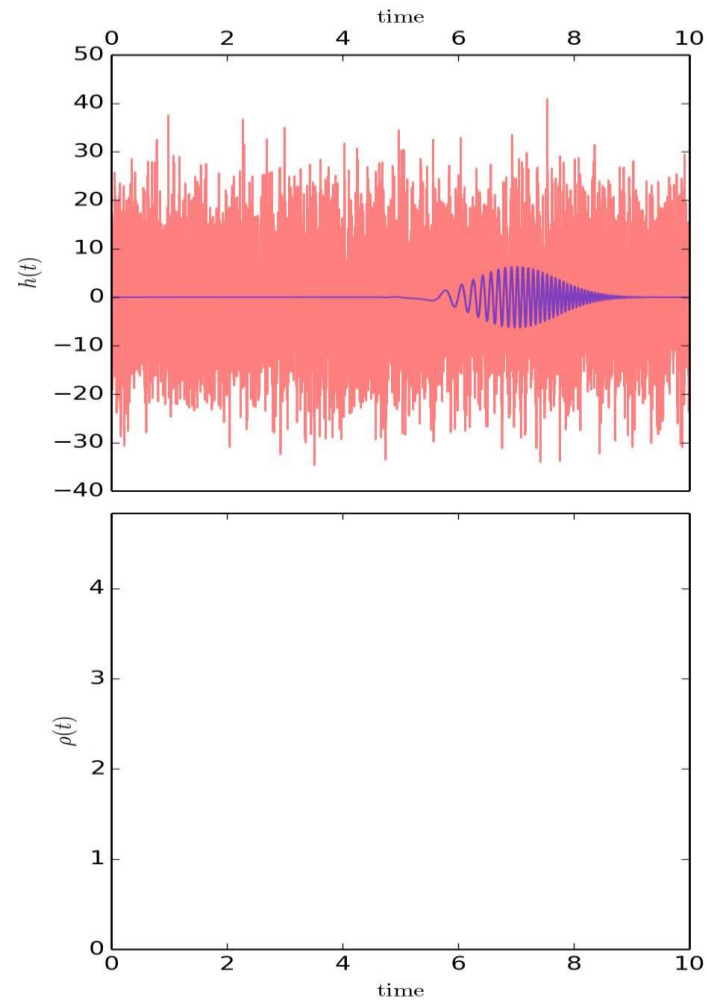


- The matched filtering is the technique used to detect GWs in this noisy data. **The idea is to model the expected signals and cross-correlate them with the data from the detector.**
- The expected GWs must be modeled: the  $h(t)$  depend on BH masses, spins, orientation etc.
- The parameter space is discretely sampled to form a template bank, containing all the modelled GW signals.
- The signal is searched through the very noisy data.

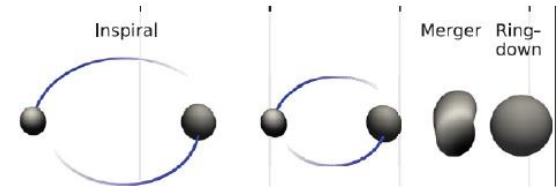
*“The signal was observed with a matched-filter signal-to-noise...”*

# Another matched templates at work

---

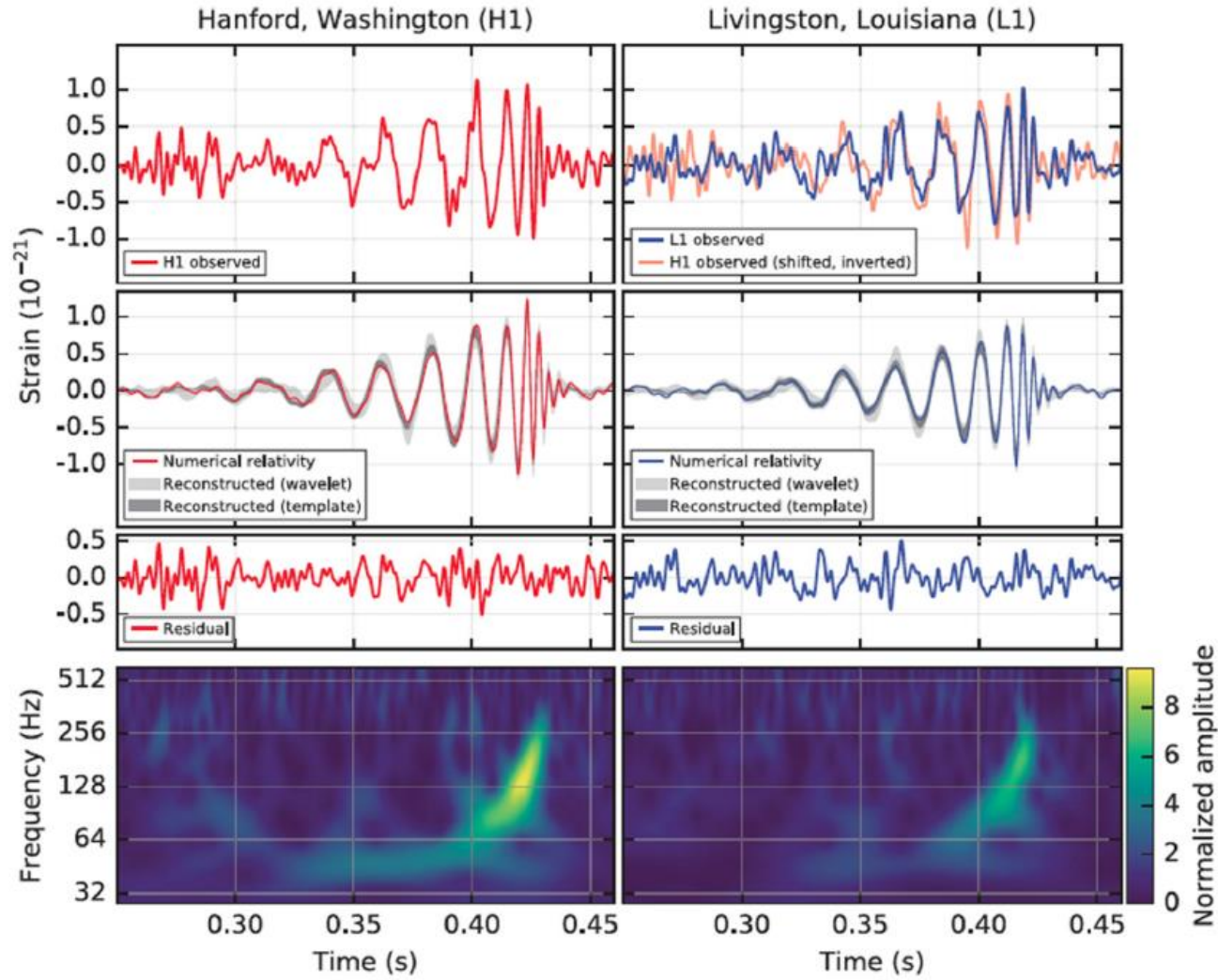


# Signal strain of the first GW



## LIGO data for GW150914

- **Top panel** shows the strain  $h$  (H/L) vs. time. Spectral noise features have been filtered.
- **Second row:** fit to the data using different waveforms. In color, the signals obtained from numerical relativity
- **Third row:** the residuals (data-fitted signal)
- **Fourth row:** time-frequency representation of the data. The frequency increasing over time (**chirp effect**)



# How to derive masses and distance?

- The discovery paper contains only one formula, relating **observables** with physical parameters (masses of the system). Let derive this equation.
- The total energy of the system

$$E_{tot} = K + U = \frac{1}{2}\mu\omega_s^2 R^2 - \frac{Gm_1 m_2}{R} = -\frac{GM\mu}{2R} = -\frac{Gm_1 m_2}{2R}. \quad (13.47)$$

- If the radius of the orbit decreases, also the total energy changes

$$\frac{dE_{tot}}{dt} = \frac{GM\mu}{2R^2} \frac{dR}{dt} = \frac{GM\mu}{2R} \frac{\dot{R}}{R} \quad (13.48)$$

- According to the Kepler's third law, also the angular velocity changes,

$$\omega_s^2 = \frac{GM}{R^3} \quad \longrightarrow \quad \frac{\dot{\omega}_s}{\omega_s} = -\frac{3}{2} \frac{\dot{R}}{R}. \quad (13.49)$$

- The energy loss rate is due to the emission of GWs

$$\frac{dE_{gw}}{dt} = -\frac{dE_{tot}}{dt} = -\frac{GM\mu}{2R} \frac{\dot{R}}{R} = \frac{GM\mu}{3R} \frac{\dot{\omega}_s}{\omega_s}. \quad (13.50)$$

- By replacing the LH side with Eq. (13.36) we obtain

$$\frac{32}{5} \frac{G}{c^5} \mu^2 R^4 \omega_s^6 = \frac{GM\mu}{3R} \frac{\dot{\omega}_s}{\omega_s}, \quad (13.51)$$

# The “chirp” mass

- We can make  $d\omega/dt$  explicit in Eq. (51) removing  $R$  by using the III Kepler law

$$\dot{\omega}_s = \frac{96 \mu \omega_s^7 (GM/\omega_s^2)^{5/3}}{5 M c^5}, \quad (13.52)$$

- and, by elevating at cube

$$\dot{\omega}_s^3 = \left(\frac{96}{5}\right)^3 \frac{G^5}{c^{15}} \mu^3 M^2 \omega_s^{11} = \left(\frac{96}{5}\right)^3 \frac{\omega_s^{11}}{c^{15}} \cdot (G\mathcal{M})^5, \quad (13.53)$$

- Were the combination of reduced and total mass is called “**chirp mass**”:

$$\mathcal{M} \equiv (\mu^3 M^2)^{1/5} = \frac{(m_1 m_2)^{3/5}}{(m_1 + m_2)^{1/5}}. \quad (13.54)$$

- The “**chirp mass**” can be derived by inverting Eq. (53)

$$\mathcal{M} = \frac{c^3}{G} \left[ \left(\frac{5}{96}\right)^3 \omega_s^{-11} \dot{\omega}_s^3 \right]^{1/5}. \quad (13.55)$$

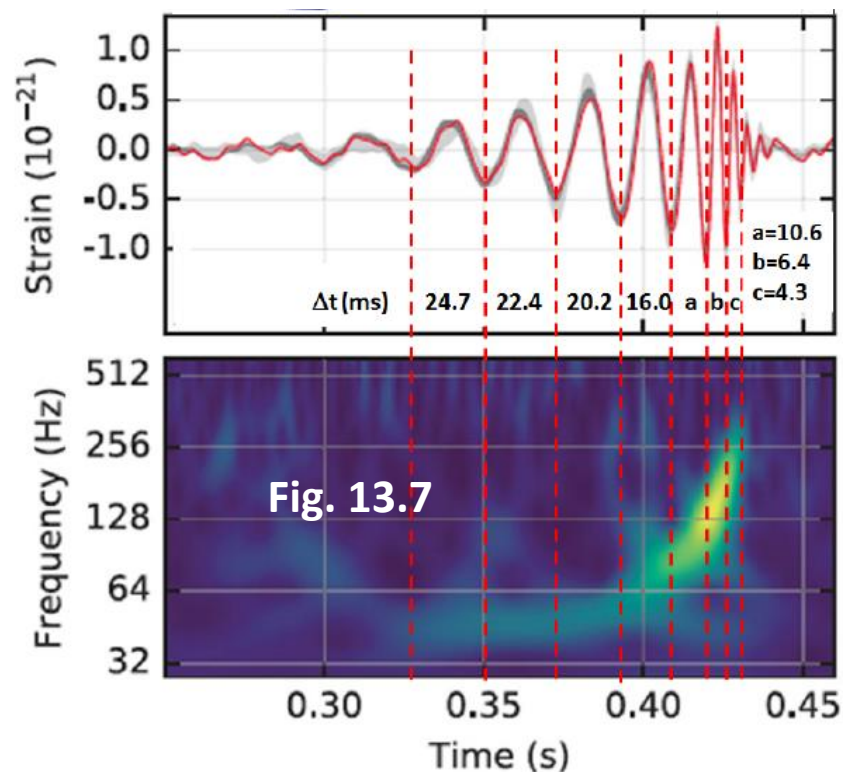
- or, in terms of the GW frequency ( $\nu_{\text{gw}} = 2\nu_s = \omega_s/\pi$ ), we obtain the equation in the discovery paper:

$$\mathcal{M} = \frac{c^3}{G} \left( \frac{5}{96} \pi^{-8/3} \nu_{\text{gw}}^{-11/3} \dot{\nu}_{\text{gw}} \right)^{3/5}, \quad (13.56)$$



# Deriving the chirp mass from data (inspiral)

- Equation (13.56) shows that as the BHs spiral inward, the frequency of the GW increases rapidly. This is the famous **chirp effect**, visible in Figs. 13.6 and 13.7.
- The chirp mass  $\mathcal{M}$  can be extracted from the values of time  $\Delta t$  between successive minima in the strain  $h(t)$  in the Figure (values in the **Table**)



$\Delta t$ (ms)	$\nu_{gw}$ (Hz)	$\dot{\nu}_{gw}$ (Hz s <sup>-1</sup> )	$\nu_{gw}^{11}$ $\dot{\nu}_{gw}^3$	$\mathcal{M}$ (kg)	$\mathcal{M}/M_{\odot}$	R (km)
24.7	40	-	-	-	-	630
22.4	45	186	4.6E-12	6.0E+31	30	590
20.2	50	241	3.2E-12	5.6E+31	28	550
16.0	63	812	9.4E-12	7.0E+31	35	470
10.6	94	3004	5.1E-12	6.2E+31	31	360
6.4	156	9673	6.7E-13	4.1E+31	21	255
4.3	233	17746	5.2E-14	2.5E+31	12	200

- Frequency =  $1/\Delta t$
- Frequency change rate,  $\Delta\nu/\Delta t$
- Term  $\nu_{gw}^{11} \dot{\nu}_{gw}^3$
- Chirp mass from eq. (56)
- Radius of the system, from Kepler III law

# Chirp mass and total mass M

- From the definitions:  $M = m_1 + m_2$

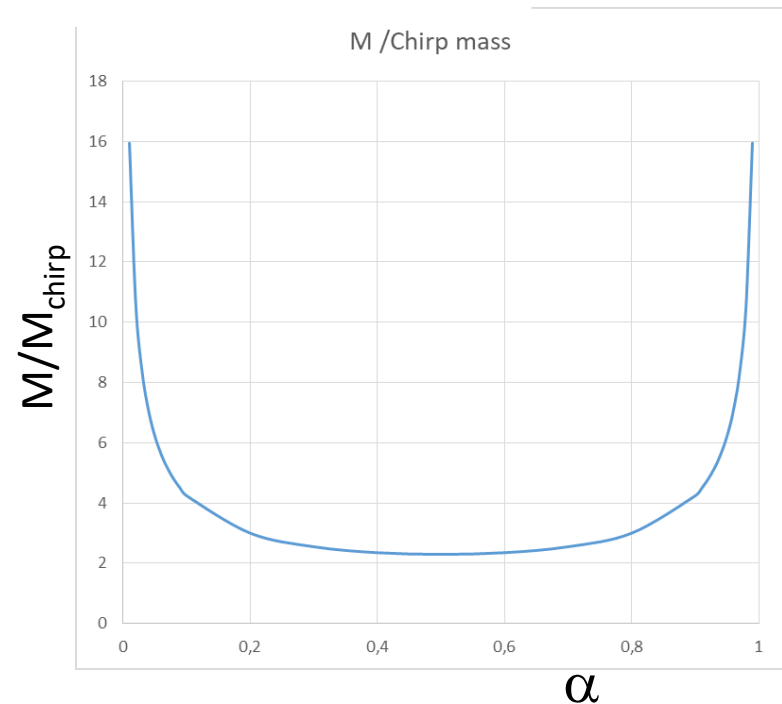
$$\mathcal{M} \equiv (\mu^3 M^2)^{1/5} = \frac{(m_1 m_2)^{3/5}}{(m_1 + m_2)^{1/5}}. \quad (13.54)$$

- If we assume:  $m_1 = \alpha M$  ;  $m_2 = (1 - \alpha)M$  , (13.57)

- Then from (54)  $M = \frac{\mathcal{M}}{[(\alpha(1 - \alpha))]^{3/5}} .$  (13.58)

- The denominator is maximum if  $\alpha=1/2$ ;  
thus M is **minimum** for  $m_1=m_2$  (equal masses)

$$M = 4^{3/5} \mathcal{M} \simeq 2.3 \mathcal{M}.$$




# Individual masses (coalescence)

- The chirp mass depends on the individual masses  $m_1, m_2$ . We need a second equation to disentangle the two values. The coalescence (*merger*) starts when the separation  $R$  between BH is equal to the Schwarzschild radius:

$$\mathcal{R} = \frac{2G}{c^2} (m_1 + m_2) . \quad (13.59)$$

- At this value of  $R$  (minimum), it corresponds the maximum angular velocity, derived again from III Kepler law:

$$\omega_s^2 = \frac{GM}{R^3} \quad \omega_{Schw} = \frac{1}{\sqrt{8}} \frac{c^3}{GM} . \quad (13.60)$$

- From inspection of Fig. 13.7:  $v_{gw}^{max} \simeq 330 \text{ Hz}$  . 

- By inverting (13.60) and using the maximum observable frequency to estimate  $\omega_{Schw}$ :

$$M = \frac{1}{\pi\sqrt{8}} \frac{c^3}{Gv_{gw}^{max}} = 1.38 \cdot 10^{32} \text{ kg} \simeq 70M_{\odot} , \quad (13.62)$$

- From the (13.58), a mass  $M=70$  solar masses corresponds to  $\alpha \approx 0.6$ , i.e. 

$$m_1^{det} = \alpha M^{det} = 42M_{\odot} \quad ; \quad m_2^{det} = (1 - \alpha)M^{det} = 28M_{\odot} . \quad (13.63)$$

- After the correction for cosmological effects (next subsection), these values are compatible with that obtained from the LIGO/Virgo Collaboration (see paper abstract).

# Exercise: luminosity distance

- The luminosity distance  $D_L$  is defined (§7.1) as the ratio between the effective luminosity of the object,  $L$ , and its energy flux,  $F$ :

$$\mathcal{F} = \frac{\mathcal{L}}{4\pi D_L^2}, \quad (7.3)$$

- For GW150914, neglecting, as a first approximation, cosmological corrections (to be verified a posteriori), and using  $F$  from (13.37) and  $L$  from (13.36), we obtain:

$$D_L^2 \frac{1}{2\pi} \frac{c^3}{G} h_o \omega_s^2 = \frac{32}{5} \frac{G}{c^5} \mu^2 R^4 \omega_s^6 \quad (13.64)$$

- and thus

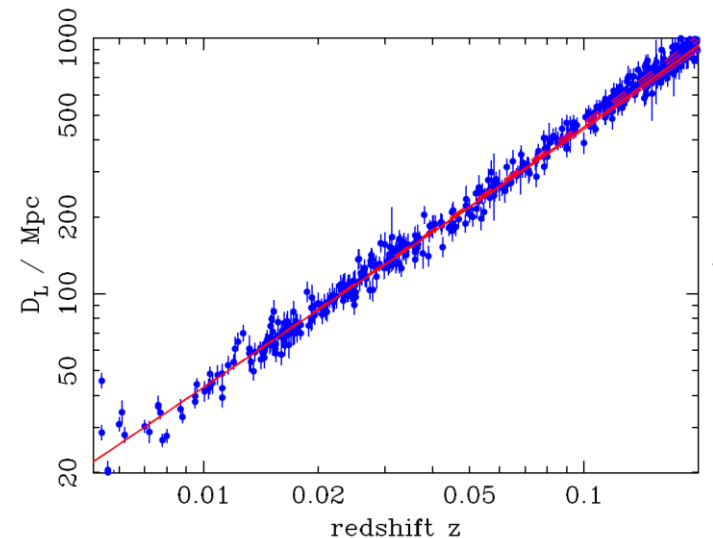
$$D_L = \frac{8}{\sqrt{5}} \frac{G}{c^4} \frac{1}{h_o} (\mu R^2 \omega_s^4). \quad (13.65)$$

- Insert the values determined in our computation for this event ( $\mu = 17 M_{\text{Sun}}$ ).
- The values of angular velocity and distance at different  $\Delta t$  are in Table 13.1, and the strain  $h_o$  in Fig. 13.7. In Eq. (13.65) we insert the values corresponding to  $\Delta t = 16.0$  ms, obtaining a value in agreement with the  $D_L = 410$  Mpc reported in the paper:

$$D_L \simeq 1.1 \cdot 10^{25} \text{ m} = 0.4 \text{ Gpc}, \quad (13.66)$$

# Exercise: Redshift and effects on observables

- Similarly to the electromagnetic radiation, GWs are stretched by the Universe expansion.
- The redshift  $z$  of an object cannot be directly measured using GWs
- If the GW source is identified through a different measurement (**multimessenger program**), the  $z$  measured with different instruments can be used.
- For GW150914), the  $z$  can be determined using standard cosmology, e.g., from Fig. 7.1.
- This increases the wavelength (at redshift  $z$ ), decreases the frequency of the waves detected (“det”) on Earth compared to their values when emitted at the source (“s”)
- time intervals are “redshifted” at the location of the observer as:  
$$\Delta t^{det} = (1+z)\Delta t^s . \quad (13.67a)$$



- this affects observable frequencies and its derivative  $dv/dt$  as:

$$v^{det} = \frac{v^s}{1+z} , \quad (13.67b)$$

$$\dot{v}^{det} = \frac{\Delta v^{det}}{\Delta t^{det}} = \frac{\Delta v^s}{\Delta t^s} \frac{1}{(1+z)^2} = \dot{v}^s \frac{1}{(1+z)^2} . \quad (13.67c)$$

# Exercise: Redshift and effects on observables

- The effect on the chirp mass at the source frame can be derived using Eq. (13.56), which correspond to the detected value:

$$\mathcal{M}^{det} \propto (\mathbf{v}_{gw}^{det})^{-11/3} (\dot{\mathbf{v}}_{gw}^{det})^{3/5} = \frac{(\mathbf{v}^s)^{-11/5}}{(1+z)^{-11/5}} \frac{(\dot{\mathbf{v}}^s)^{3/5}}{(1+z)^{6/5}} = (1+z)(\mathbf{v}^s)^{-11/5} (\dot{\mathbf{v}}^s)^{3/5}$$

$$\mathcal{M}^{det} = (1+z)\mathcal{M}^s . \quad (13.68)$$

- and similarly for constituent masses:

$$m_1^{det} = (1+z)m_1 \quad ; \quad m_2^{det} = (1+z)m_2 , \quad (13.69)$$

- Direct inspection of the detector data yields mass values from the red-shifted waves, and thus the values we derived in (13.63) must be scaled down by  $(1+z)$  to obtain the values at the source frame (those reported in the abstract of the paper).
- In conclusion, from the derived redshift of  $z \approx 0.1$ , the masses at the source frame are about 10% smaller than that derived in (13.63) at the detector frame.



# Total emitted energy as GWs

---

- Another impressive observation of GW150914 is the surprising amount of energy emitted in the form of gravitational radiation.
- Initial very large distance of the black holes,  $R \rightarrow \infty$ , and a final separation given by the sum of their Schwarzschild radii

$$\Delta E = E_{tot}^f - E_{tot}^i = -\frac{Gm_1m_2}{2\mathcal{R}} = -\frac{Gm_1m_2c^2}{4GM} = \frac{\mu c^2}{4} \simeq 4M_{\odot}c^2 \quad (13.70)$$

- in agreement with the value of  $3Mc^2$  determined in GW150914 paper. Equation (13.70) also shows that, for a fixed total mass  $M = m_1 + m_2$ , the radiated energy depends on the reduced mass  $\mu$ , and thus it is maximum when the merging BH masses are equal.

## Spin of the BH

- The BHs spin leads to additional velocity-dependent interactions during inspiral. Incorporation of these effects is not straightforward
- For an object with mass  $m$  and spin  $\mathbf{S}$ , the dimensionless spin is

$$\chi = \frac{c}{G} \frac{|\mathbf{S}|}{m^2}. \quad (13.71)$$

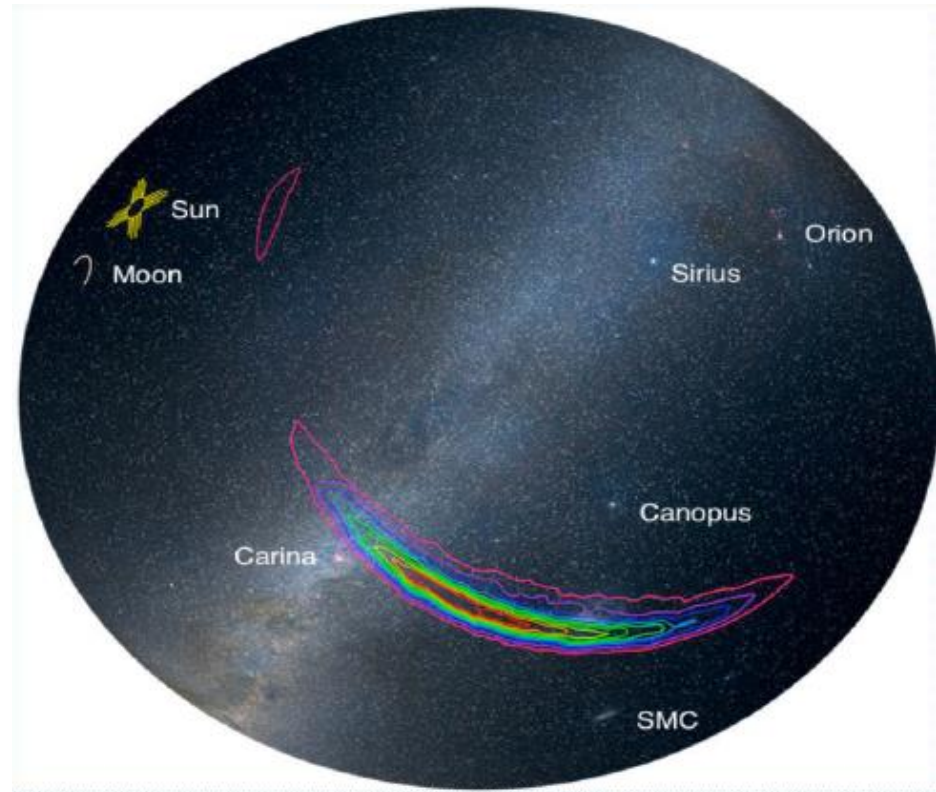
- The spin modify the radius of the event horizon with respect to the Schwarzschild radius (smaller for  $\chi \rightarrow 1$ )

# GW Localization

- Interferometers are linearly-polarized quadrupolar detectors and do not have good directional sensitivity.
- As a result, two antennas are necessary in order to obtain minimum directional information on the source position using the relative arrival time of the signal.
- For a distance  $L=3000$  km and  $\lambda=1.5 \times 10^6$  m (200 Hz), LIGO has a resolution of

$$\Delta\theta \simeq \frac{\lambda}{L} = 0.5 \text{ rad} \sim 28^\circ .$$

- The uncertainty on the source position corresponds to about  $\Delta\theta^2 \approx 800 \text{ deg}^2$ .
- The 90% credible region mentioned in paper corresponds to approximately  $600 \text{ deg}^2$ .
- The localization improves significantly using three detectors (by a factor of  $\sim 10$ ), as demonstrated with the GW detected in combination with VIRGO



# Status of BH-BH observations after O1 and O2\*

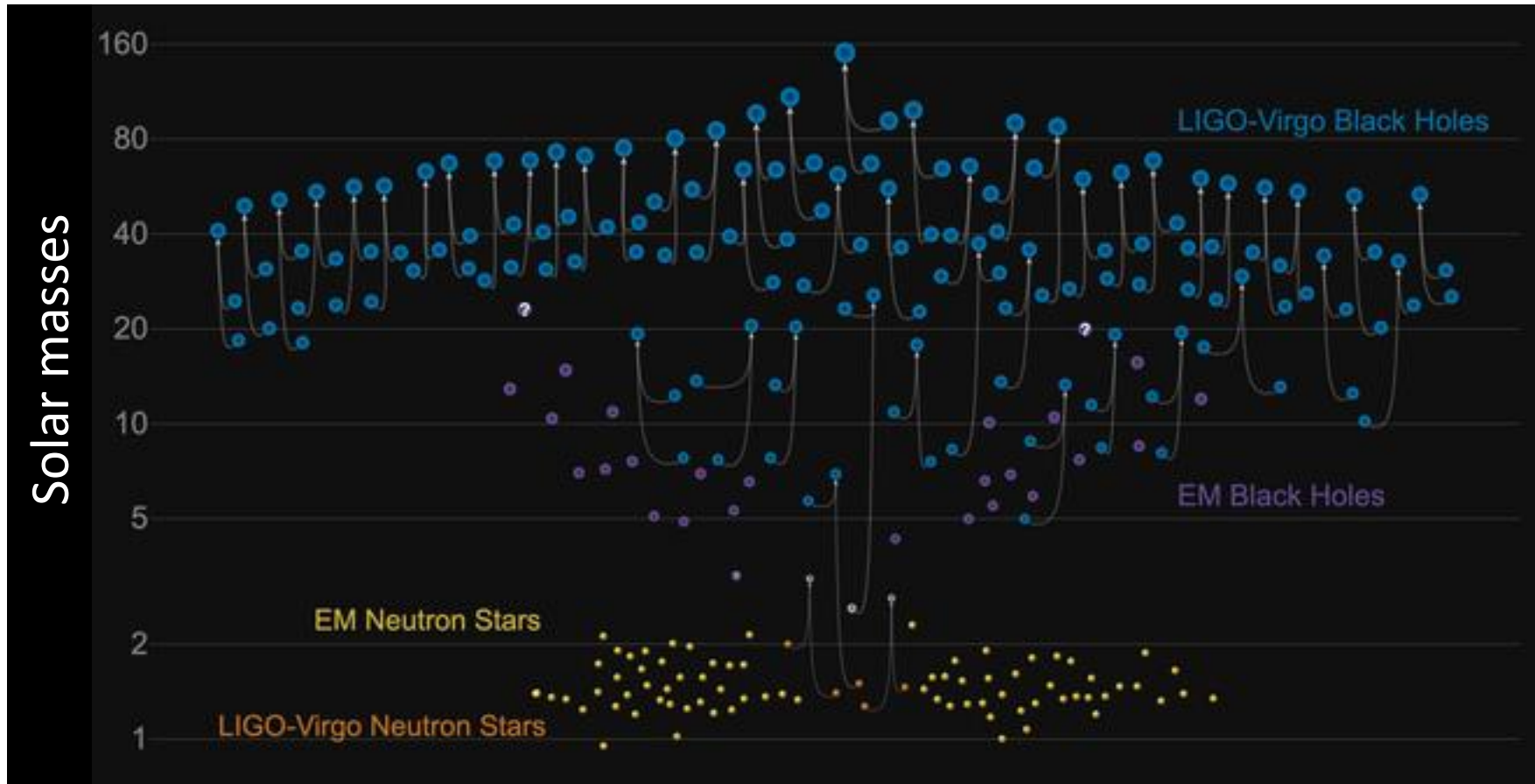
arXiv:1811.12907 and arXiv:1811.12940

Event	$m_1/M_\odot$	$m_2/M_\odot$	$M/M_\odot$	$\chi_{\text{eff}}$	$M_f/M_\odot$	$a_f$	$E_{\text{rad}}/(M_\odot c^2)$	$\ell_{\text{peak}}/(\text{erg s}^{-1})$	$d_L/\text{Mpc}$	$z$	$\Delta\Omega/\text{deg}^2$
GW150914	$35.6^{+4.8}_{-3.0}$	$30.6^{+3.0}_{-4.4}$	$28.6^{+1.6}_{-1.5}$	$-0.01^{+0.12}_{-0.13}$	$63.1^{+3.3}_{-3.0}$	$0.69^{+0.05}_{-0.04}$	$3.1^{+0.4}_{-0.4}$	$3.6^{+0.4}_{-0.4} \times 10^{56}$	$430^{+150}_{-170}$	$0.09^{+0.03}_{-0.03}$	179
GW151012	$23.3^{+14.0}_{-5.5}$	$13.6^{+4.1}_{-4.8}$	$15.2^{+2.0}_{-1.1}$	$0.04^{+0.28}_{-0.19}$	$35.7^{+9.9}_{-3.8}$	$0.67^{+0.13}_{-0.11}$	$1.5^{+0.5}_{-0.5}$	$3.2^{+0.8}_{-1.7} \times 10^{56}$	$1060^{+540}_{-480}$	$0.21^{+0.09}_{-0.09}$	1555
GW151226	$13.7^{+8.8}_{-3.2}$	$7.7^{+2.2}_{-2.6}$	$8.9^{+0.3}_{-0.3}$	$0.18^{+0.20}_{-0.12}$	$20.5^{+6.4}_{-1.5}$	$0.74^{+0.07}_{-0.05}$	$1.0^{+0.1}_{-0.2}$	$3.4^{+0.7}_{-1.7} \times 10^{56}$	$440^{+180}_{-190}$	$0.09^{+0.04}_{-0.04}$	1033
GW170104	$31.0^{+7.2}_{-5.6}$	$20.1^{+4.9}_{-4.5}$	$21.5^{+2.1}_{-1.7}$	$-0.04^{+0.17}_{-0.20}$	$49.1^{+5.2}_{-3.9}$	$0.66^{+0.08}_{-0.10}$	$2.2^{+0.5}_{-0.5}$	$3.3^{+0.6}_{-0.9} \times 10^{56}$	$960^{+430}_{-410}$	$0.19^{+0.07}_{-0.08}$	924
GW170608	$10.9^{+5.3}_{-1.7}$	$7.6^{+1.3}_{-2.1}$	$7.9^{+0.2}_{-0.2}$	$0.03^{+0.19}_{-0.07}$	$17.8^{+3.2}_{-0.7}$	$0.69^{+0.04}_{-0.04}$	$0.9^{+0.0}_{-0.1}$	$3.5^{+0.4}_{-1.3} \times 10^{56}$	$320^{+120}_{-110}$	$0.07^{+0.02}_{-0.02}$	396
GW170729	$50.6^{+16.6}_{-10.2}$	$34.3^{+9.1}_{-10.1}$	$35.7^{+6.5}_{-4.7}$	$0.36^{+0.21}_{-0.25}$	$80.3^{+14.6}_{-10.2}$	$0.81^{+0.07}_{-0.13}$	$4.8^{+1.7}_{-1.7}$	$4.2^{+0.9}_{-1.5} \times 10^{56}$	$2750^{+1350}_{-1320}$	$0.48^{+0.19}_{-0.20}$	1033
GW170809	$35.2^{+8.3}_{-6.0}$	$23.8^{+5.2}_{-5.1}$	$25.0^{+2.1}_{-1.6}$	$0.07^{+0.16}_{-0.16}$	$56.4^{+5.2}_{-3.7}$	$0.70^{+0.08}_{-0.09}$	$2.7^{+0.6}_{-0.6}$	$3.5^{+0.6}_{-0.9} \times 10^{56}$	$990^{+320}_{-380}$	$0.20^{+0.05}_{-0.07}$	340
GW170814	$30.7^{+5.7}_{-3.0}$	$25.3^{+2.9}_{-4.1}$	$24.2^{+1.4}_{-1.1}$	$0.07^{+0.12}_{-0.11}$	$53.4^{+3.2}_{-2.4}$	$0.72^{+0.07}_{-0.05}$	$2.7^{+0.4}_{-0.3}$	$3.7^{+0.4}_{-0.5} \times 10^{56}$	$580^{+160}_{-210}$	$0.12^{+0.03}_{-0.04}$	87
GW170817	$1.46^{+0.12}_{-0.10}$	$1.27^{+0.09}_{-0.09}$	$1.186^{+0.001}_{-0.001}$	$0.00^{+0.02}_{-0.01}$	$\leq 2.8$	$\leq 0.89$	$\geq 0.04$	$\geq 0.1 \times 10^{56}$	$40^{+10}_{-10}$	$0.01^{+0.00}_{-0.00}$	16
GW170818	$35.5^{+7.5}_{-4.7}$	$26.8^{+4.3}_{-5.2}$	$26.7^{+2.1}_{-1.7}$	$-0.09^{+0.18}_{-0.21}$	$59.8^{+4.8}_{-3.8}$	$0.67^{+0.07}_{-0.08}$	$2.7^{+0.5}_{-0.5}$	$3.4^{+0.5}_{-0.7} \times 10^{56}$	$1020^{+430}_{-360}$	$0.20^{+0.07}_{-0.07}$	39
GW170823	$39.6^{+10.0}_{-6.6}$	$29.4^{+6.3}_{-7.1}$	$29.3^{+4.2}_{-3.2}$	$0.08^{+0.20}_{-0.22}$	$65.6^{+9.4}_{-6.6}$	$0.71^{+0.08}_{-0.10}$	$3.3^{+0.9}_{-0.8}$	$3.6^{+0.6}_{-0.9} \times 10^{56}$	$1850^{+840}_{-840}$	$0.34^{+0.13}_{-0.14}$	1651

- 11 GW observed in O1 and O2 (values with 90% C.L.). All are BBH, a part GW170817.
- For BBH events the  $z$  was calculated from the luminosity distance and assumed cosmology.
- The columns show source masses  $m_i$  and **chirp mass  $M$** , dimensionless effective aligned **spin  $\chi_{\text{eff}}$** , final source frame mass  $M_f$ , final spin  $\alpha_f$ , radiated energy  $E_{\text{rad}}$ , peak luminosity  $\ell_{\text{peak}}$ , luminosity distance  $d_L$ , redshift  $z$  and sky localization  $\Delta\Omega$  (90% credible region).

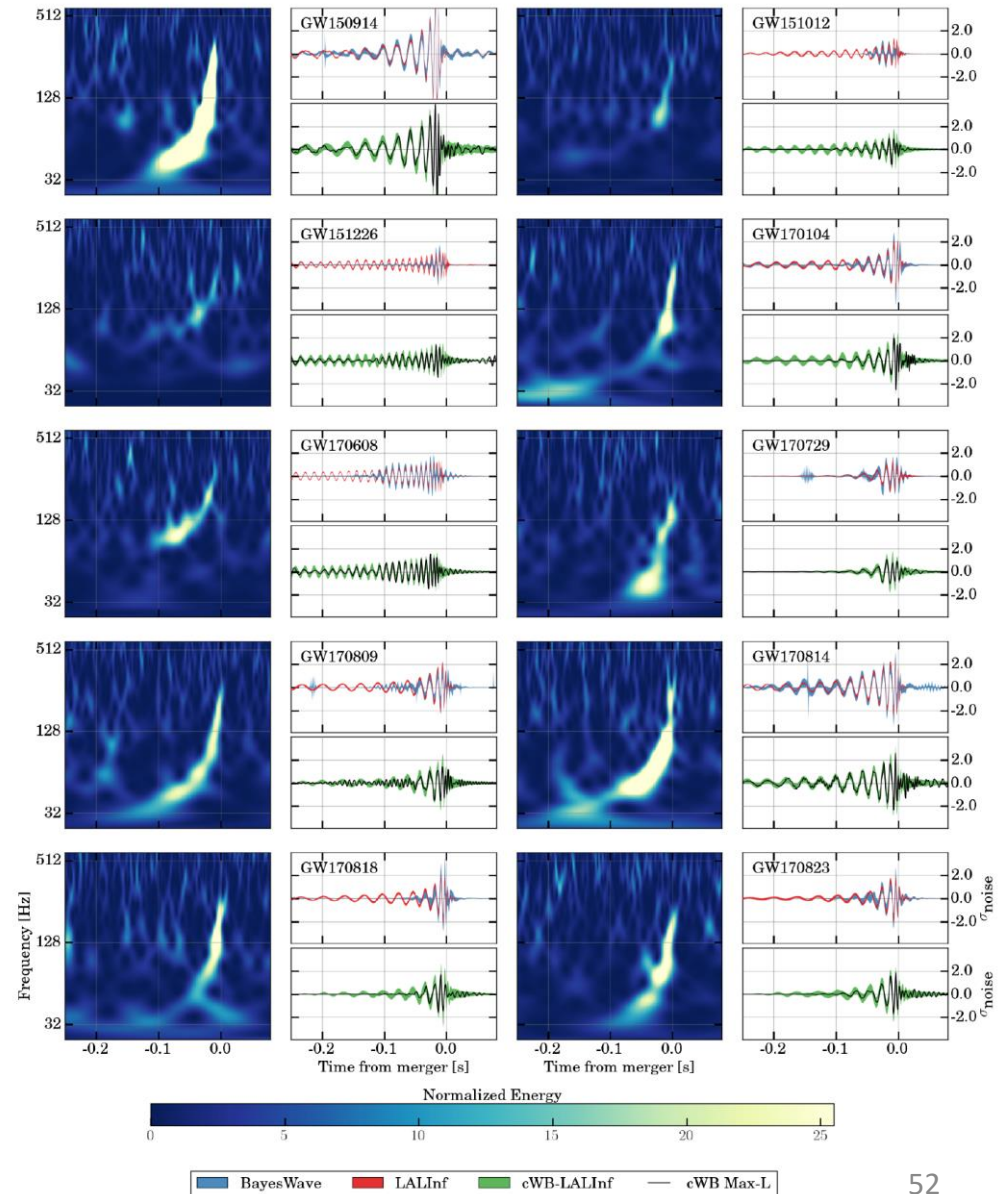
# Masses of observed stellar BHs and NS

- ~ 20 of stellar BHs indirectly detected via EM radiation (as X-rays);
- The largest was  $15 M_{\odot}$ ; the more likely mass was 5-10  $M_{\odot}$ ;
- All BHs detected using GWs have masses larger than expected (apart two events)
- **The simple distribution of BH masses (initial and final) require a complete revision of astrophysical models of stellar evolution.**



# Stellar BHs observed in O1, O2

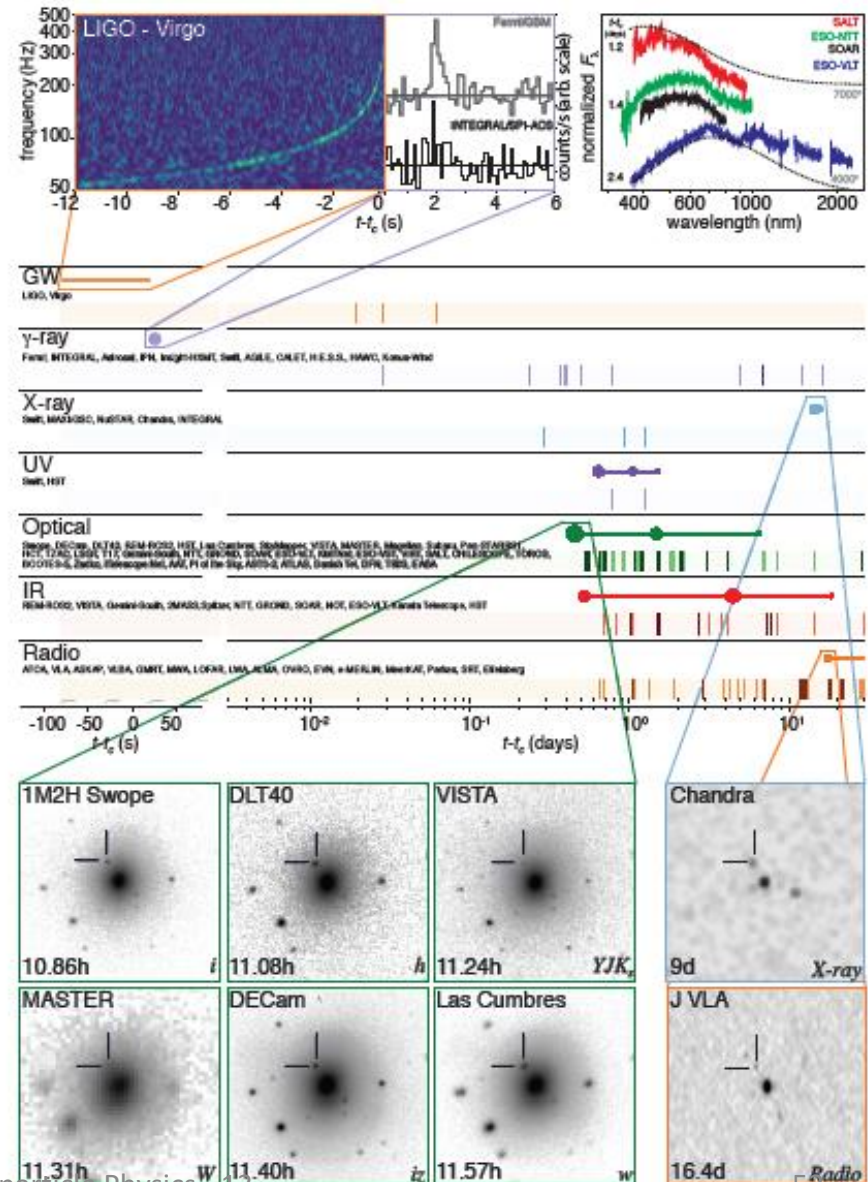
- Time-frequency maps and reconstructed signal waveforms for the ten BBH events





# August, 17th 2017: a long series of events

- If sufficiently close to the Earth, the merger of two neutron stars (NSs) is predicted to produce three observable phenomena:
  - a **gravitational wave (GW)** signal;
  - a **short GRB** and, possibly, neutrinos;
  - a transient **optical-near-infrared** source.
- Such a transient (also called a “**kilonova**”) would be powered by the synthesis of large amounts of very heavy elements such as Au and Pt via rapid neutron capture (the so-called astrophysical r-process, Sect. 12.16).

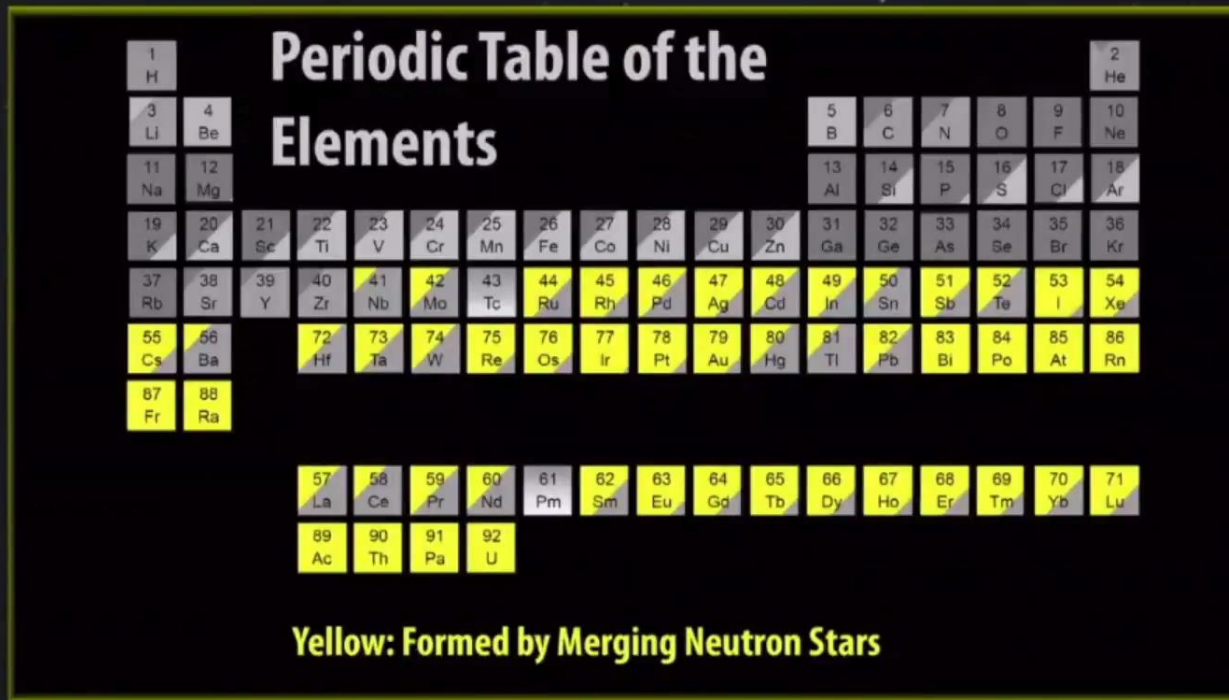


# August, 17th 2017: a long series of events

a gold mine for physics

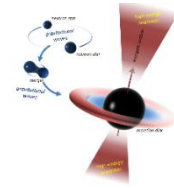
New Gravitational Wave Discovery (Press Conference and Online Q&A Session)

Press release October 16th 2017



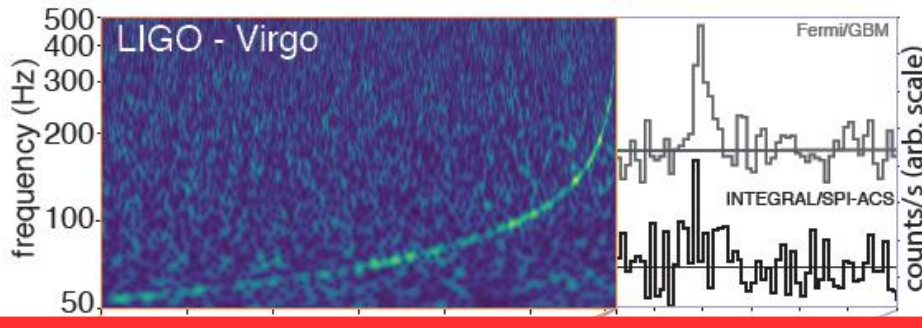


# Time-sequence of observations (I)

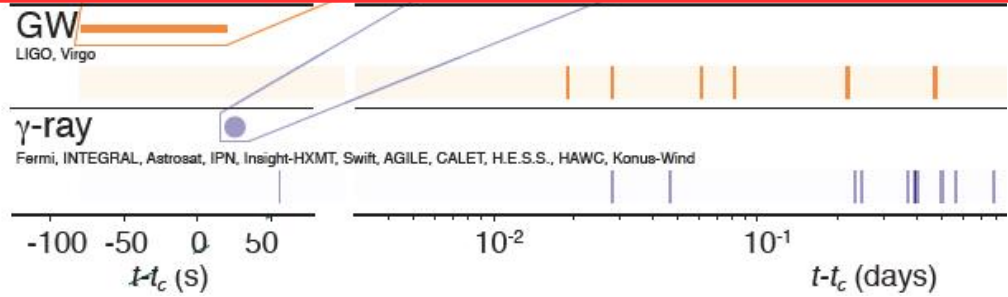


- GRB170817A

- Fermi-GBM 17Aug 12:41:20 UTC 12:41:06 UTC , 1100 deg<sup>2</sup>, D=?



**$\Delta T = 1.734 \text{ s} : \text{GRB170817A} = \text{GW170817}$**



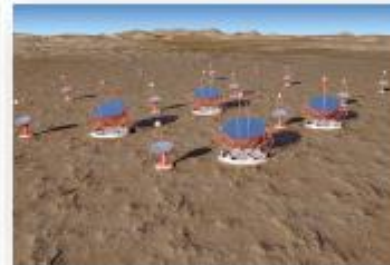
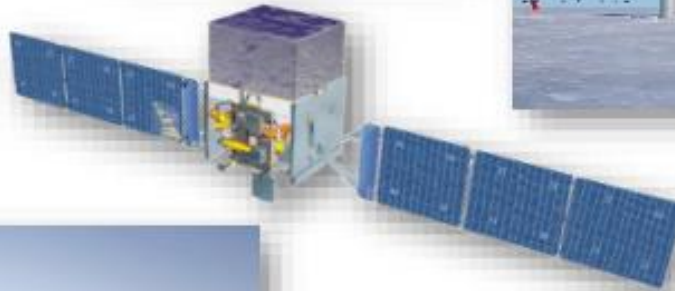
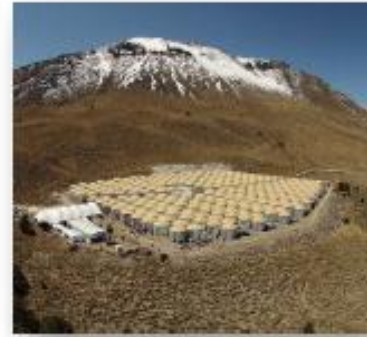
- GW170817

- LIGO (online) 17Aug 13:21:42 UTC 12:41:04 UTC
  - LIGO/VIRGO 17Aug 17:54:51 UTC 12:41:04 UTC, 31deg<sup>2</sup>, 40 Mpc

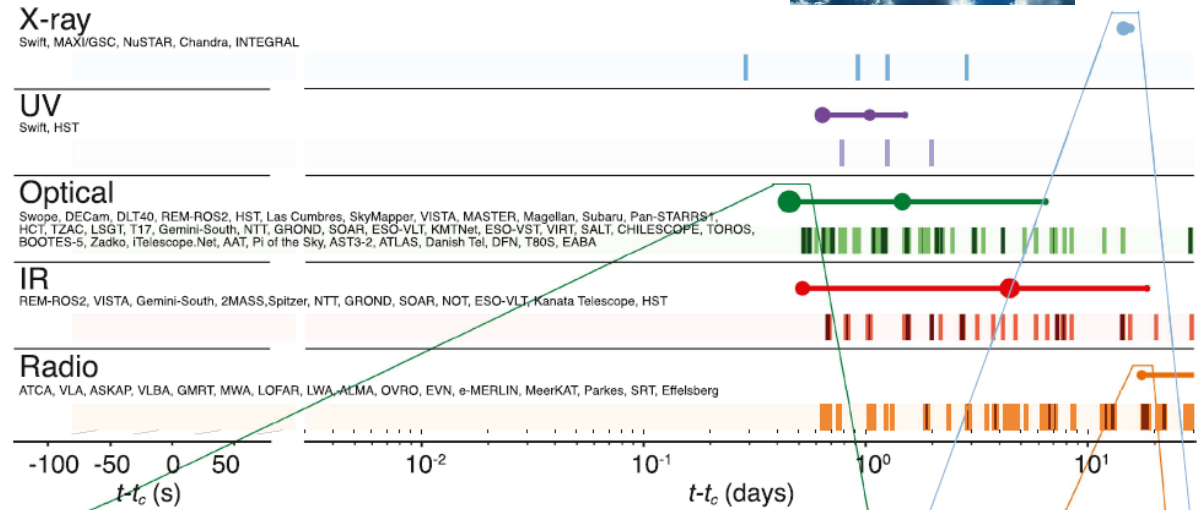
# The response of the astrophysical community

---

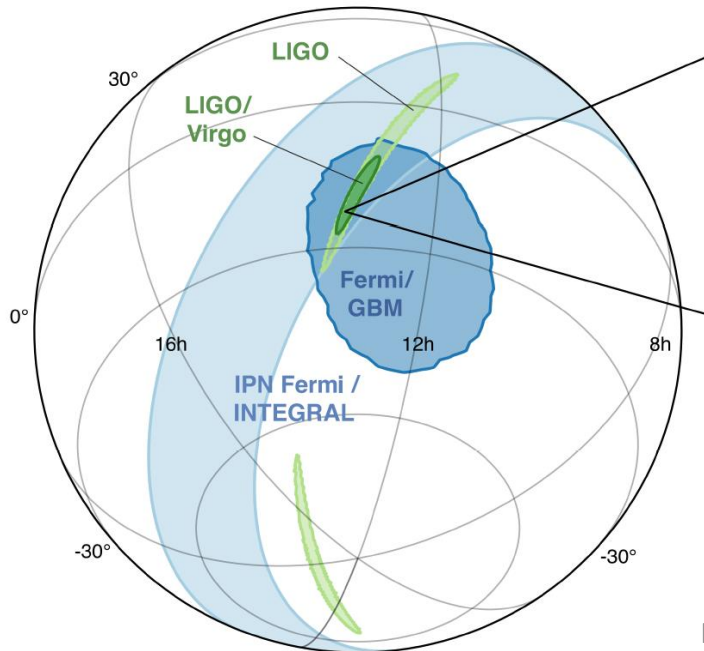
friends 80+



# Time-sequence of observations (II)



MMA — LIGO-P1700294-v4



- No neutrinos
  - IceCube 14:05:11 UTC
  - ANTARES 20:35:31 UTC
- No prompt X-ray
  - MAXI 17:21:54 UPC
- No prompt radio



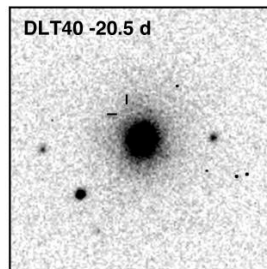
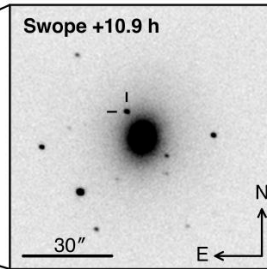
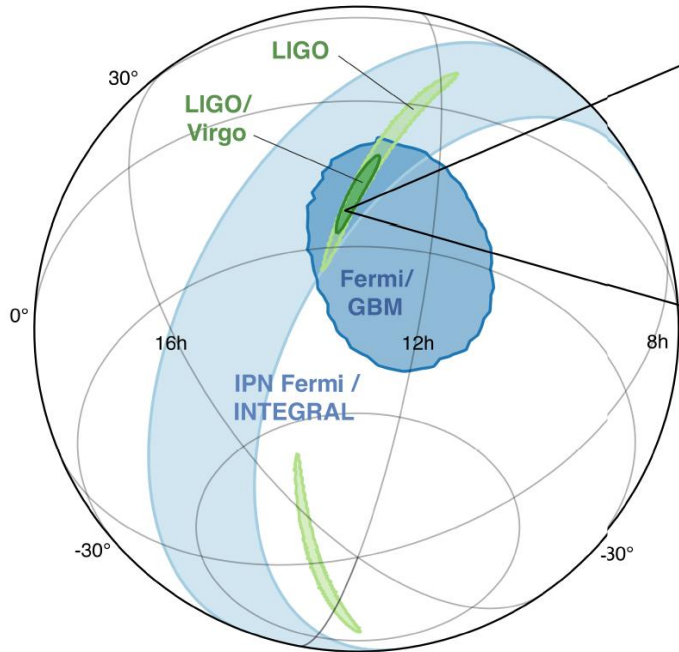
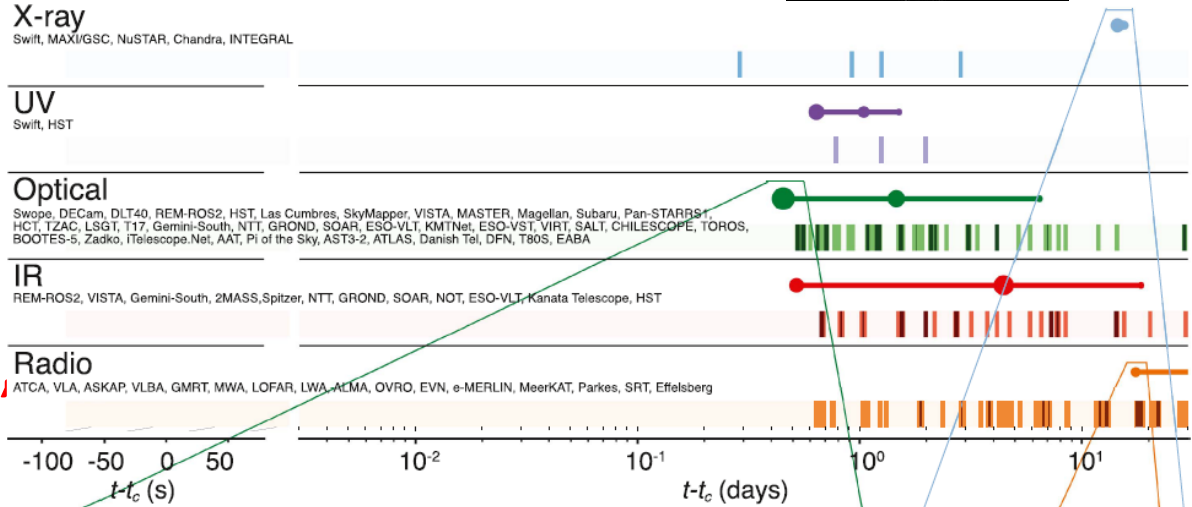
# Time-sequence of observations (III)



- AT2017gfo (IAU designation)
  - Swope SN Survey (Cile) 18 Aug 01:05 UTC
  - Others, after few min/h

**RA=13<sup>h</sup>09<sup>m</sup>48<sup>s</sup>, δ=-23°22'**  
**NGC 4993, 40 Mpc**

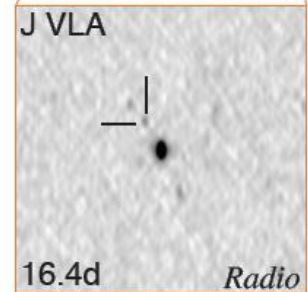
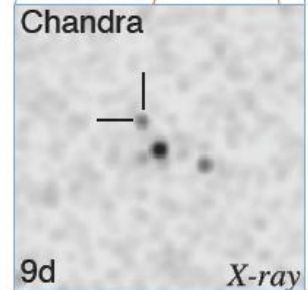
MMA — LIGO-P1700294-v4



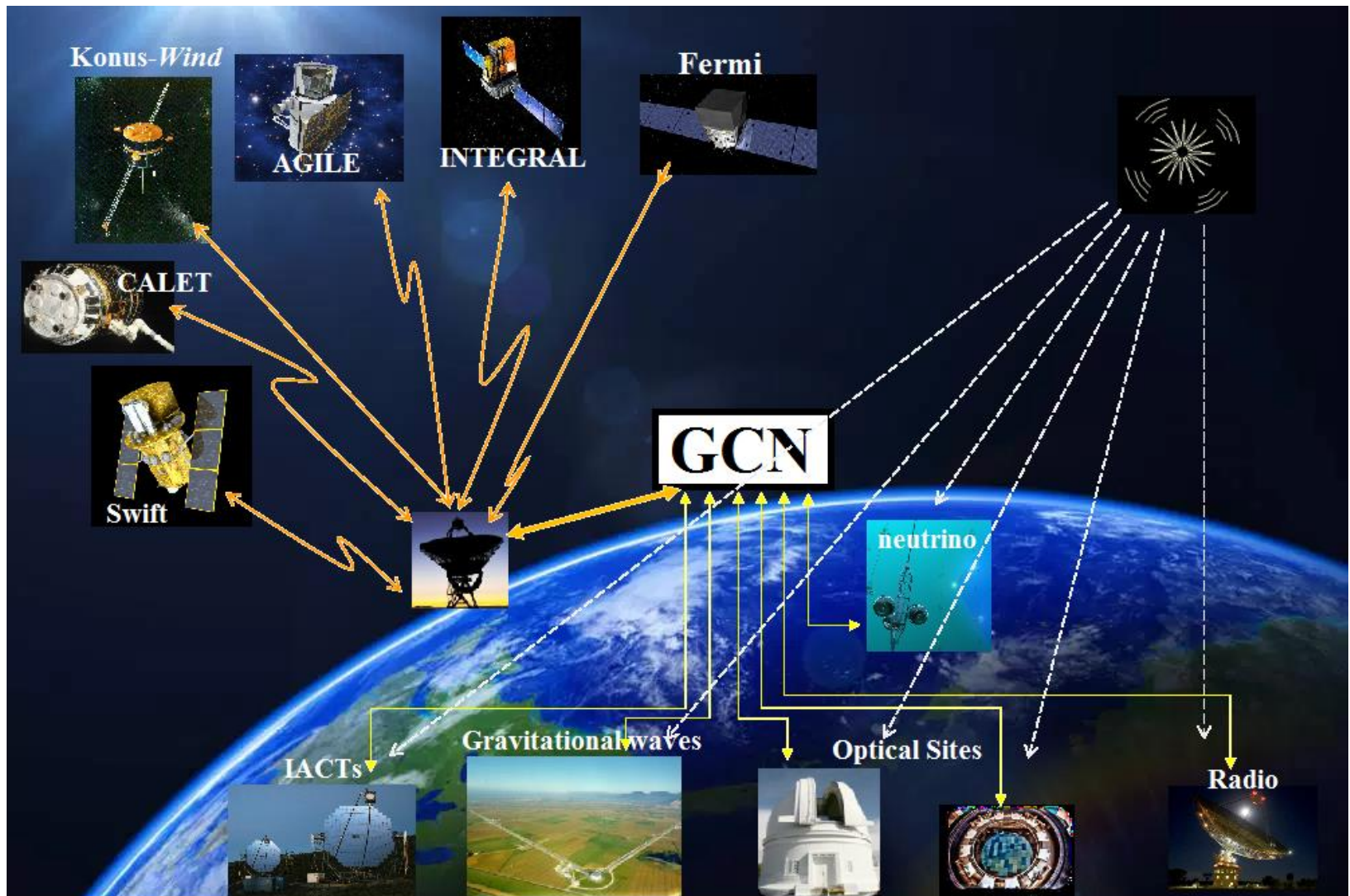
Optic

X-rays

Radio



# The communication network



# The «Multimessenger» paper

THE ASTROPHYSICAL JOURNAL LETTERS, 848:L12 (59pp), 2017 October 20

© 2017, The American Astronomical Society. All rights reserved.

**OPEN ACCESS**

<https://doi.org/10.3847/2041-8213/aa91c9>



## Multi-messenger Observations of a Binary Neutron Star Merger

LIGO Scientific Collaboration and Virgo Collaboration, Fermi GBM, INTEGRAL, IceCube Collaboration, AstroSat Cadmium Zinc Telluride Imager Team, IPN Collaboration, The Insight-Hxmt Collaboration, ANTARES Collaboration, The Swift Collaboration, AGILE Team, The 1M2H Team, The Dark Energy Camera GW-EM Collaboration and the DES Collaboration, The DLT40 Collaboration, GRAVITA: GRAVitational Wave Inaf TeAm, The Fermi Large Area Telescope Collaboration, ATCA: Australia Telescope Compact Array, ASKAP: Australian SKA Pathfinder, Las Cumbres Observatory Group, OzGrav, DWF (Deeper, Wider, Faster Program), AST3, and CAASTRO Collaborations, The VINROUGE Collaboration, MASTER Collaboration, J-GEM, GROWTH, JAGWAR, Caltech-NRAO, TTU-NRAO, and NuSTAR Collaborations, Pan-STARRS, The MAXI Team, TZAC Consortium, KU Collaboration, Nordic Optical Telescope, ePESSTO, GROND, Texas Tech University, SALT Group, TOROS: Transient Robotic Observatory of the South Collaboration, The BOOTES Collaboration, MWA: Murchison Widefield Array, The CALET Collaboration, IKI-GW Follow-up Collaboration, H.E.S.S. Collaboration, LOFAR Collaboration, LWA: Long Wavelength Array, HAWC Collaboration, The Pierre Auger Collaboration, ALMA Collaboration, Euro VLBI Team, Pi of the Sky Collaboration, The Chandra Team at McGill University, DFN: Desert Fireball Network, ATLAS, High Time Resolution Universe Survey, RIMAS and RATIR, and SKA South Africa/MeerKAT (See the end matter for the full list of authors.)

*Received 2017 October 3; revised 2017 October 6; accepted 2017 October 6; published 2017 October 16*

### Abstract

On 2017 August 17 a binary neutron star coalescence candidate (later designated GW170817) with merger time 12:41:04 UTC was observed through gravitational waves by the Advanced LIGO and Advanced Virgo detectors. The *Fermi* Gamma-ray Burst Monitor independently detected a gamma-ray burst (GRB 170817A) with a time delay of  $\sim 1.7$  s with respect to the merger time. From the gravitational-wave signal, the source was initially localized to a sky region of  $31 \text{ deg}^2$  at a luminosity distance of  $40_{-8}^{+8}$  Mpc and with component masses consistent with neutron stars. The component masses were later measured to be in the range  $0.86$  to  $2.26 M_{\odot}$ . An extensive observing campaign was launched across the electromagnetic spectrum leading to the discovery of a bright optical transient (SSS17a, now with the IAU identification of AT 2017gfo) in NGC 4993 (at  $\sim 40$  Mpc) less than 11 hours after the merger by the One-Meter, Two Hemisphere (1M2H) team using the 1 m Swope Telescope. The optical transient was independently detected by multiple teams within an hour. Subsequent observations targeted the object and its environment. Early ultraviolet observations revealed a blue transient that faded within 48 hours. Optical and infrared observations showed a redward evolution over  $\sim 10$  days. Following early non-detections, X-ray and radio emission were discovered at the transient's position  $\sim 9$  and  $\sim 16$  days, respectively, after the merger. Both the X-ray and radio emission likely arise from a physical process that is distinct from the one that powers the UV/optical/infrared emission. No

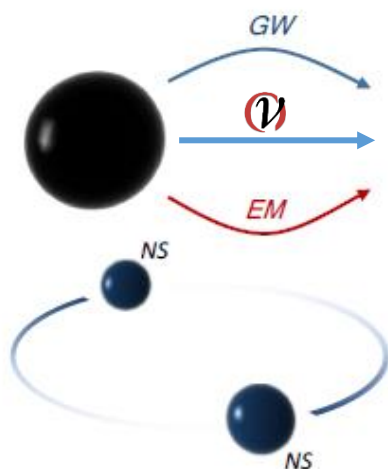






# Key points of the discovery

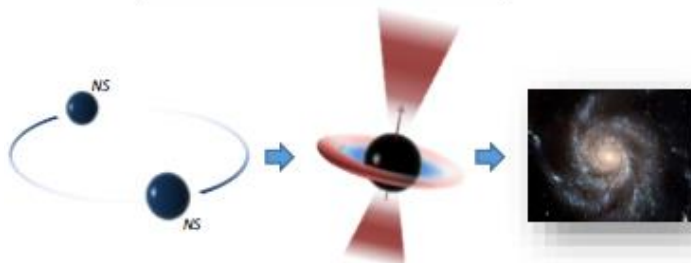
## PHYSICS



**Speed of gravity  
(speed of neutrinos)**

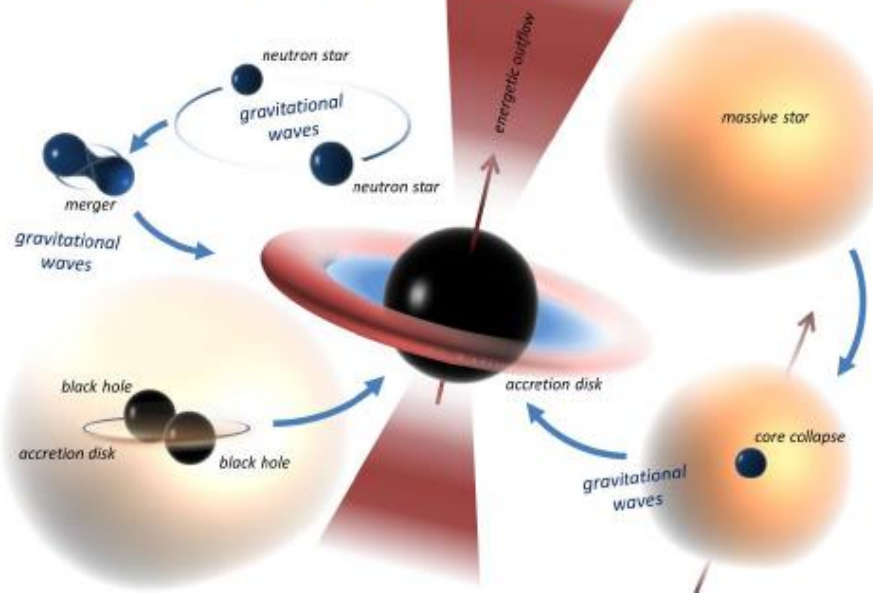
**EoS of nuclear matter .**

## COSMOLOGY



- Ladder scale
- Measure  $H_0$
- Test of  $\Lambda$ CDM

## ASTROPHYSICS

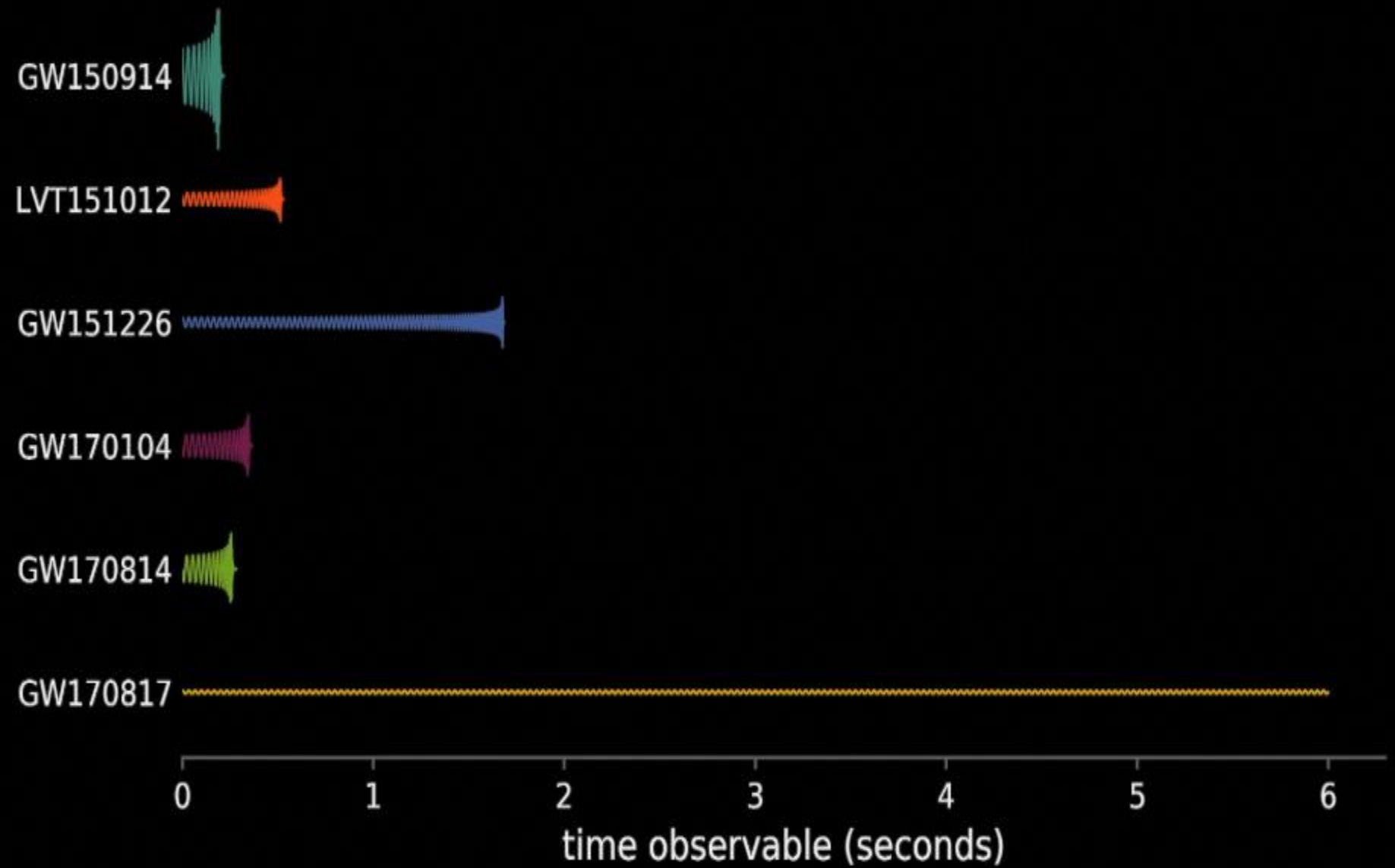


- Short GRB
- Heavy elements production sites (r-process)
- Accretion disks in astrophysics
- Jets
- UHECRs Acceleration
- Neutrino production
- Formation of binary systems
- Formation of black holes

# GW170817: NS coalescence

---

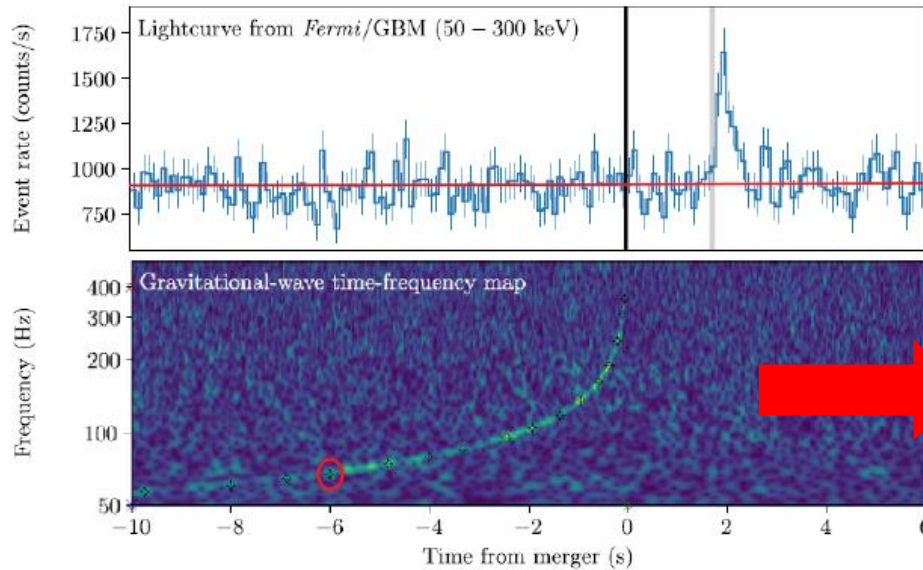




LIGO/Virgo/University of Oregon/Ben Farr

# Parameter of the system from GW170817

- Chirp mass from (13.56) 

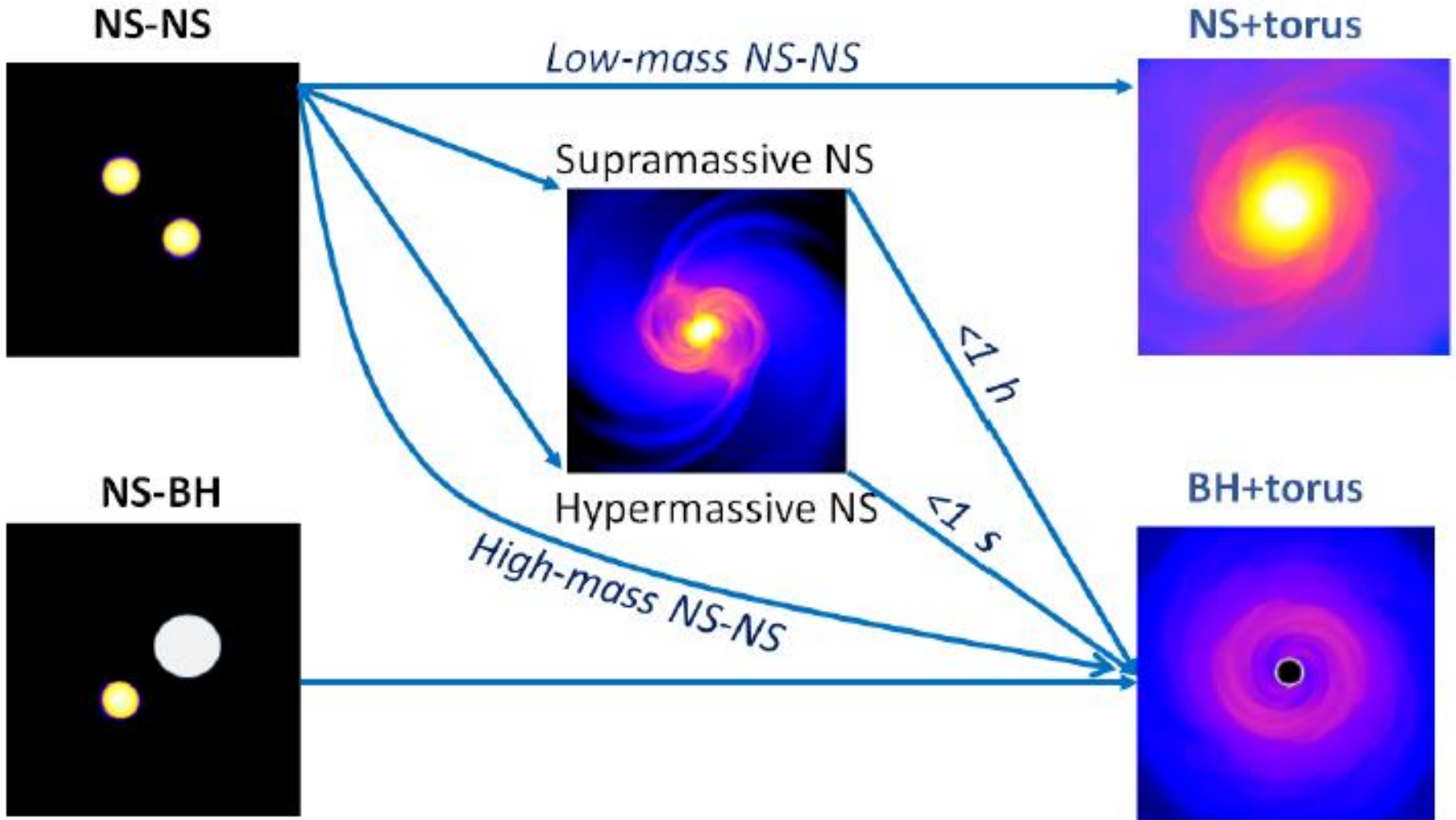


$\Delta t$ (s)	$\nu_{gw}$ (Hz)	$\dot{\nu}_{gw}$ (Hz s <sup>-1</sup> )	$\mathcal{M}$ (kg)	$\mathcal{M}/M_{\odot}$	R (km)
-9.74	57.1	-	-	-	166
-6.87	64.8	2.7	2.1E+30	1.0	153
-4.83	74.3	4.7	2.2E+30	1.1	140
-3.33	85.7	7.6	2.1E+30	1.1	127
-2.45	95.7	11.4	2.1E+30	1.1	118
-1.93	104.7	17.2	2.2E+30	1.1	111
-1.37	118.2	23.8	2.1E+30	1.0	102
-0.94	136.3	42.8	2.1E+30	1.1	93
-0.59	163.1	75.1	2.0E+30	1.0	83
-0.21	239.7	201.1	1.6E+30	0.8	64
-0.06	359.9	810.0	1.5E+30	0.7	49

	$ \chi_{NS}  < 0.05$	$ \chi_{NS}  < 0.89$
Chirp mass $\mathcal{M}$	$1.188^{+0.004}_{-0.002} M_{\odot}$	$1.188^{+0.004}_{-0.002} M_{\odot}$
Luminosity distance $D_L$	$40^{+8}_{-14}$ Mpc	$40^{+8}_{-14}$ Mpc
Mass ratio $q = m_2/m_1$	0.7-1.0	0.4-1.0
Total mass $M = m_1 + m_2$	$2.74^{+0.04}_{-0.01} M_{\odot}$	$2.82^{+0.47}_{-0.09} M_{\odot}$
Primary mass $m_1$	1.36-1.60 $M_{\odot}$	1.36-2.26 $M_{\odot}$
Secondary mass $m_2$	1.17-1.36 $M_{\odot}$	0.86-1.36 $M_{\odot}$
Viewing angle $\Theta$	$\leq 55^{\circ}$	$\leq 56^{\circ}$
Using NGC 4993 location	$\leq 28^{\circ}$	$\leq 28^{\circ}$
Tidal deformability $\Lambda(1.4M_{\text{odot}})$	$\leq 800$	$\leq 1400$
Radiated energy $E_{\text{rad}}$	$> 0.025 M_{\odot} c^2$	$> 0.025 M_{\odot} c^2$

Parameters of the system from the paper

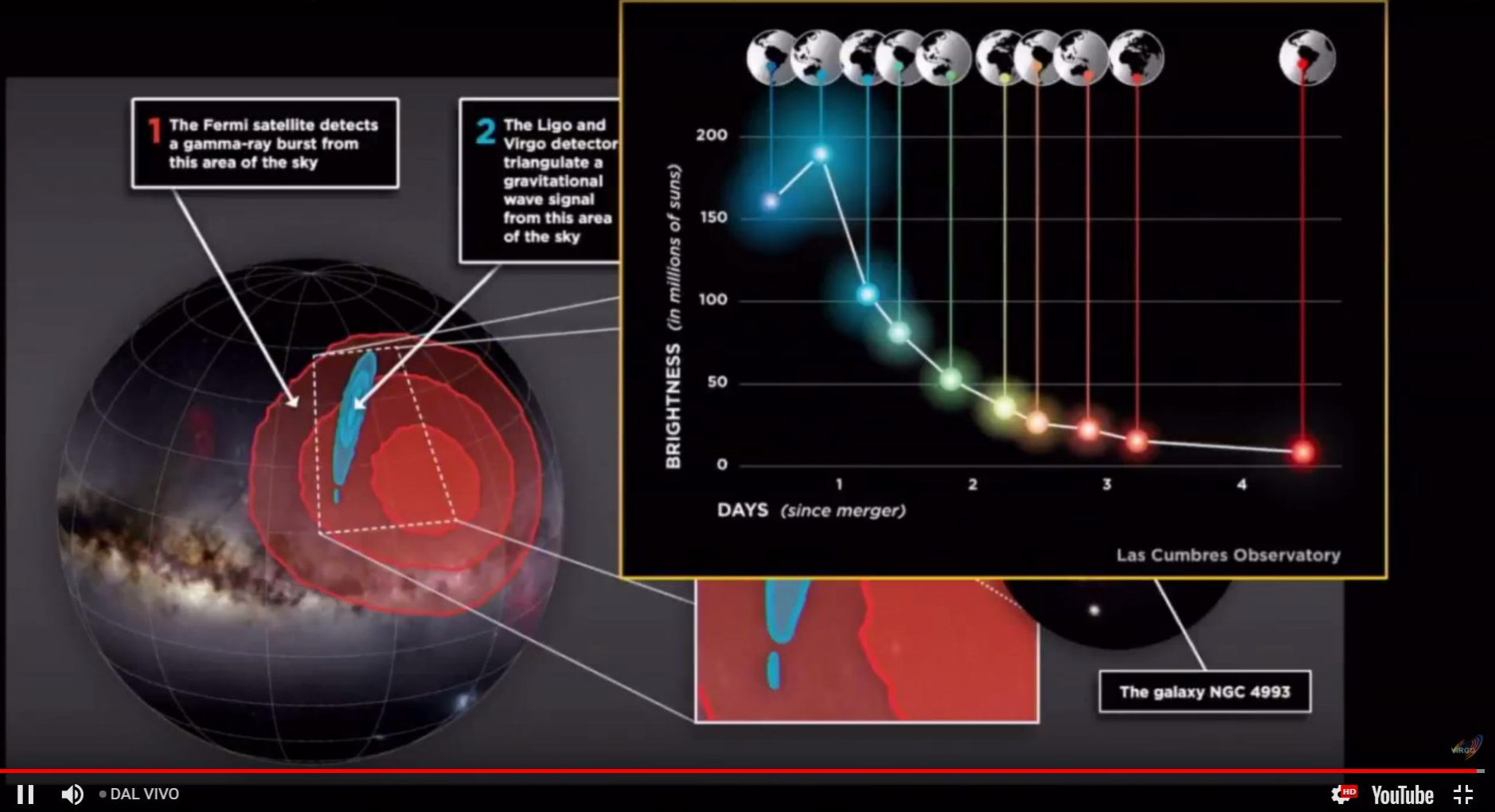
# Final state: NS or BH?





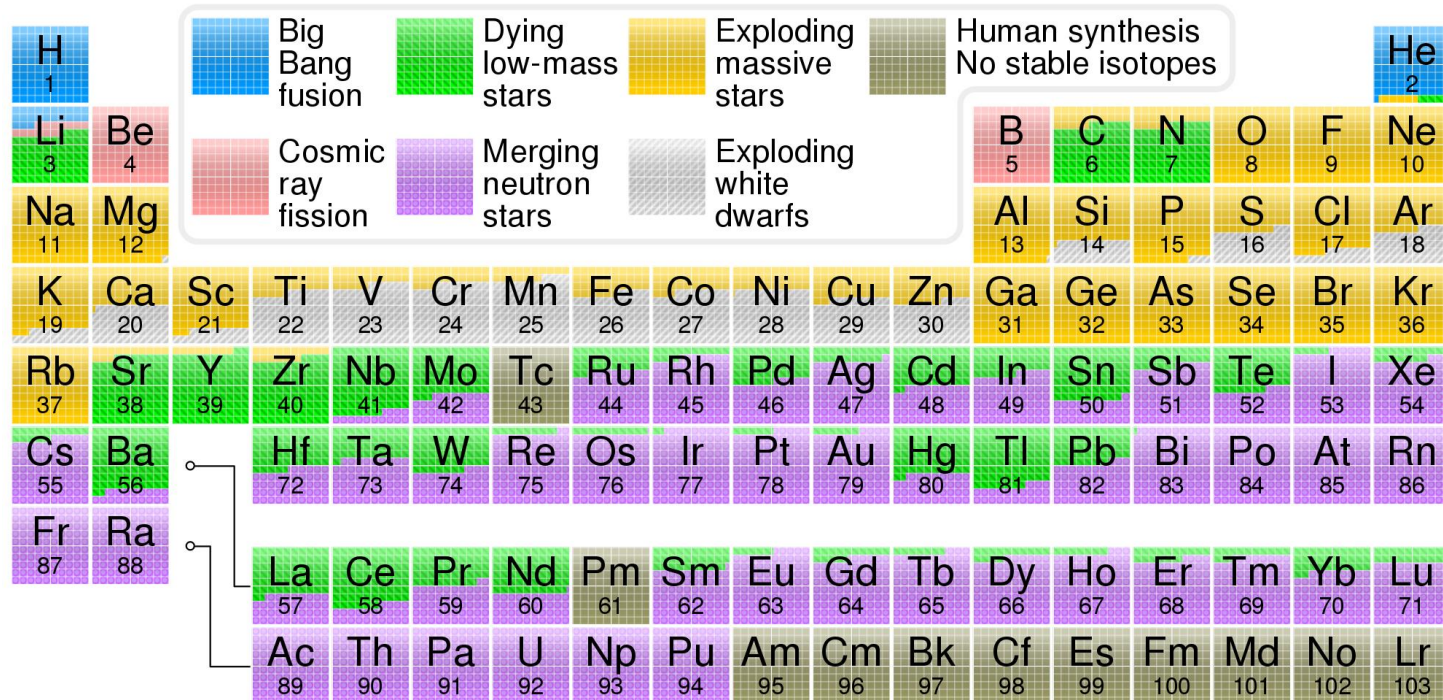
# The EM follow-up

New Gravitational Wave Discovery (Press Conference and Online Q&A Session)



# The Origin of Trans-Fe Elements

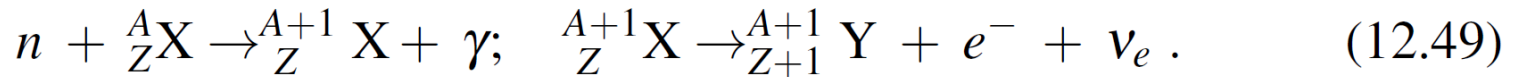
- Elements of higher mass number become progressively rarer, because they increasingly absorb energy in being produced.
- The abundance of elements in the Solar System is thought to be similar (Chap. 3)
- Supernova nucleosynthesis is the theory of the releasing in the Universe of elements up to iron ( $Z = 26$ ) and nickel ( $Z = 28$ ) in supernova explosions (F. Hoyle, 1954).
- Core-collapse supernovae are the main contributors of the heavy elements ( $A \geq 12$ )  
Elements heavier than iron are produced by neutron capture in neutron-rich



# Slow (s) and Rapid (r) processes

---

- Elements heavier than iron are produced by neutron capture in neutron-rich astrophysical environments, followed by  $\beta$  decay of the forming nuclei.



- The so-called **s-process** is believed to occur mostly in asymptotic giant.
- The s-process is believed to occur over time scales of thousands of years, passing decades between successive neutron captures.
- The **r-process** also involves neutron capture, as in (12.49) but the neutron capture time is much smaller than the nucleus decay time, due to the high neutron density.
- The newly formed nucleus does not decay immediately; after subsequent captures, the isotopes move away from the stability valley:  $\frac{A}{Z}\text{X} \rightarrow \frac{A+1}{Z}\text{X} \rightarrow \frac{A+2}{Z}\text{X} \rightarrow \dots$
- The r-process occurs in astrophysical locations where there is a high density of free neutrons (astrophysical regions matter of ongoing researches).
- Until the observation of GW170817, the environment around core-collapse SN was the most plausible candidate.
- GW170817 showed that the most suited ambient for r-processes is probably the neutron-rich matter in a binary neutron star merger (the so-called kilonova).

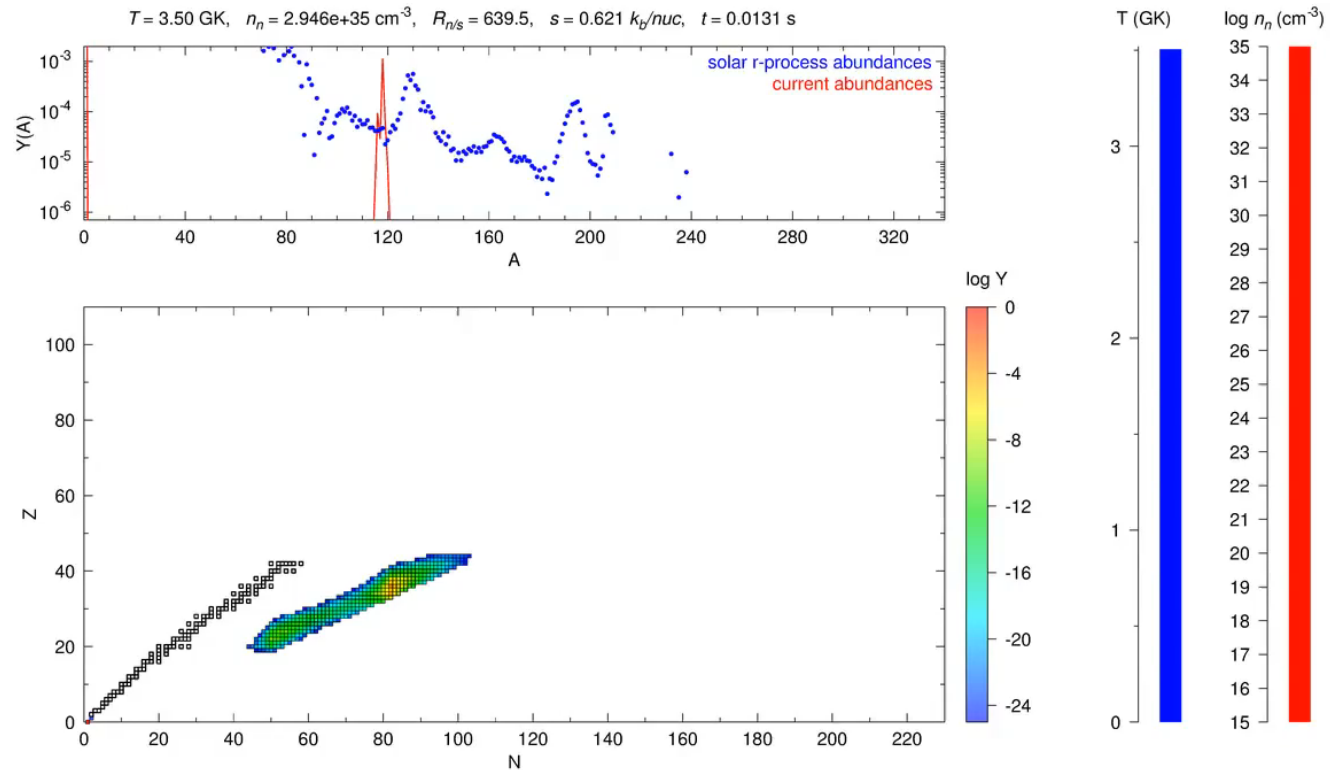
# Numerical simulation

## Electromagnetic counterparts of compact object mergers powered by the radioactive decay of *r*-process nuclei

B. D. Metzger,<sup>1\*</sup> G. Martínez-Pinedo,<sup>2</sup> S. Darbha,<sup>3</sup> E. Quataert,<sup>3</sup> A. Arcones,<sup>2,4</sup>  
D. Kasen,<sup>5</sup> R. Thomas,<sup>6</sup> P. Nugent,<sup>6</sup> I. V. Panov<sup>7,8,9</sup> and N. T. Zinner<sup>10</sup>

### *r*-process (*rapid*)

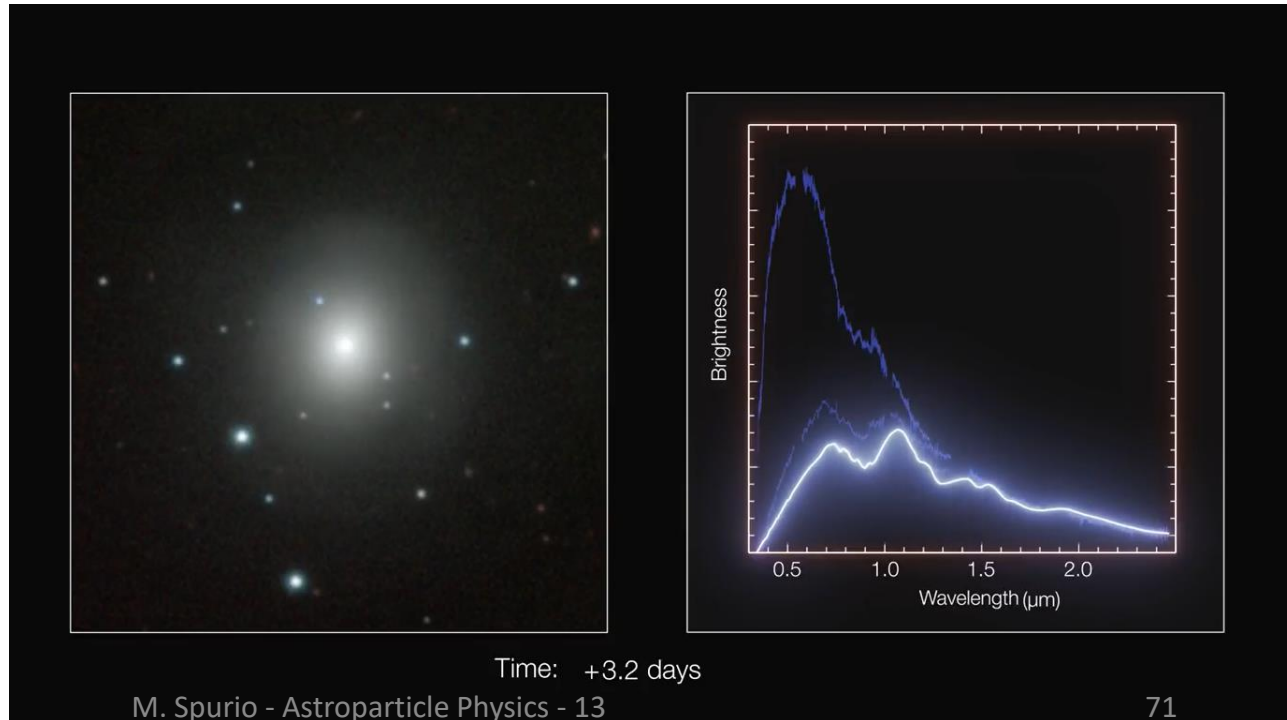
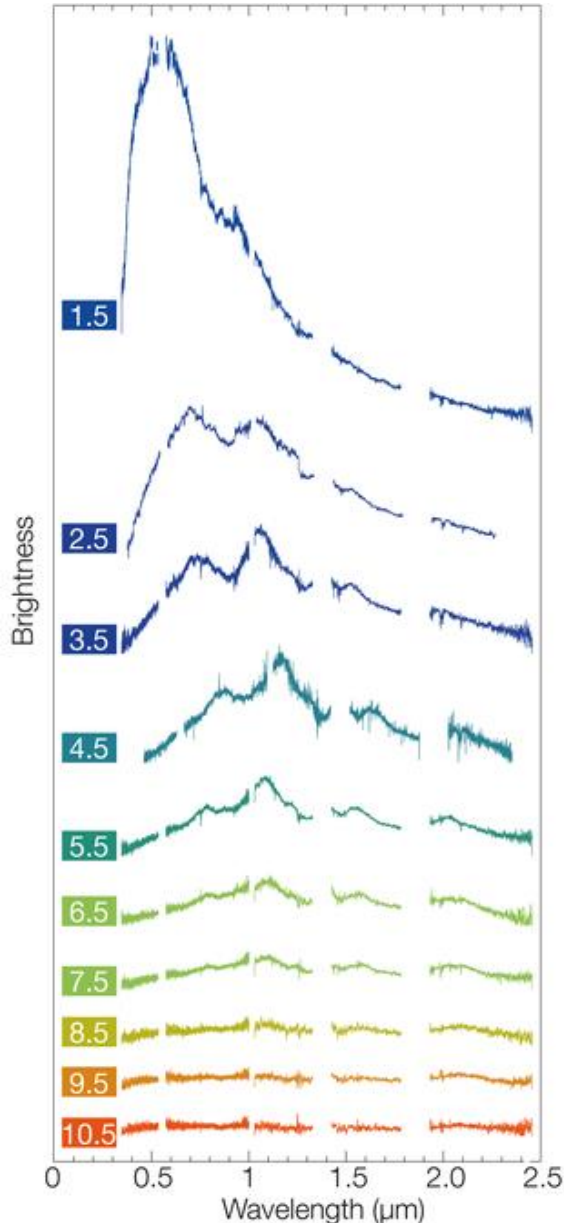
- occurs in very neutron-rich environment,
  - Supernovae?
  - Neutron star merging?
- adds many neutrons *rapidly*, before the nucleus has time to decay
- Very *n*-rich nuclei are initially unstable, thus decay to stable isotopes via  $\beta$  decay that decay converts a “*n*” into a “*p*”
- The mass number, *A*, is unchanged, while *Z* increases





# The “kilonova”

- A kilonova is a transient event observable with traditional astronomical methods occurring when two NSs merge
- The term *kilonova* (or *macronova* or *r-process supernova*) was introduced to characterize the peak brightness of the isotropic emission which reaches  $10^3$  times that of a nova.
- These observations support the hypothesis that a kilonova powered by the radioactive decay of r-process nuclei synthesized in the ejecta was produced.





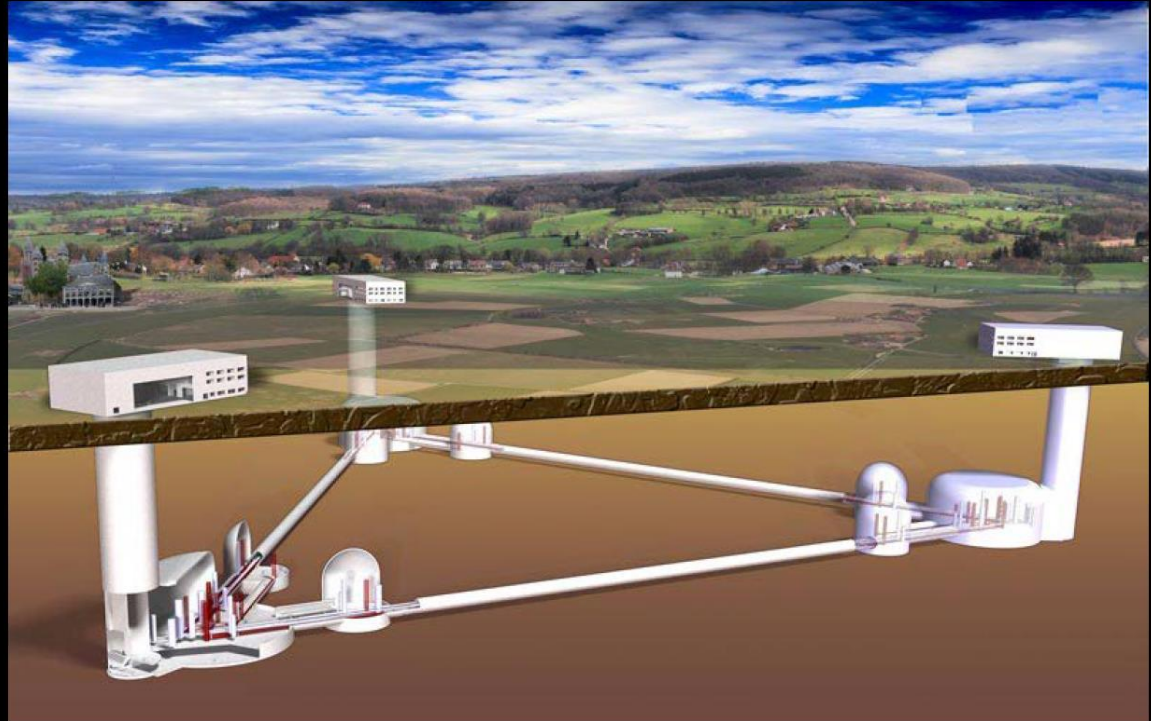
# Proposed 3rd Generation Detectors

---

## Einstein Telescope 10 km

The Einstein Telescope: x10 aLIGO

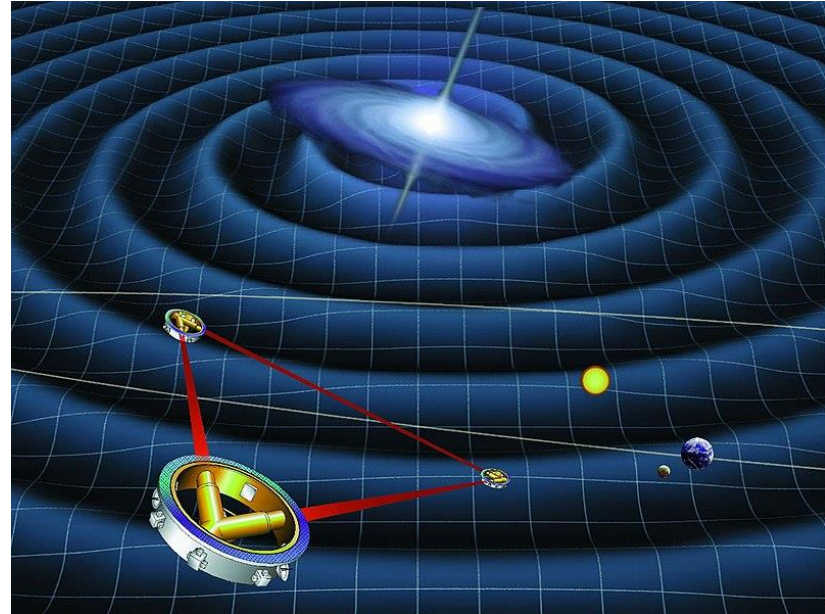
- Deep Underground;
- 10 km arms
- Triangle (polarization)
- Cryogenic
- Low frequency configuration
- high frequency configuration



# The LISA interferometer in space

---

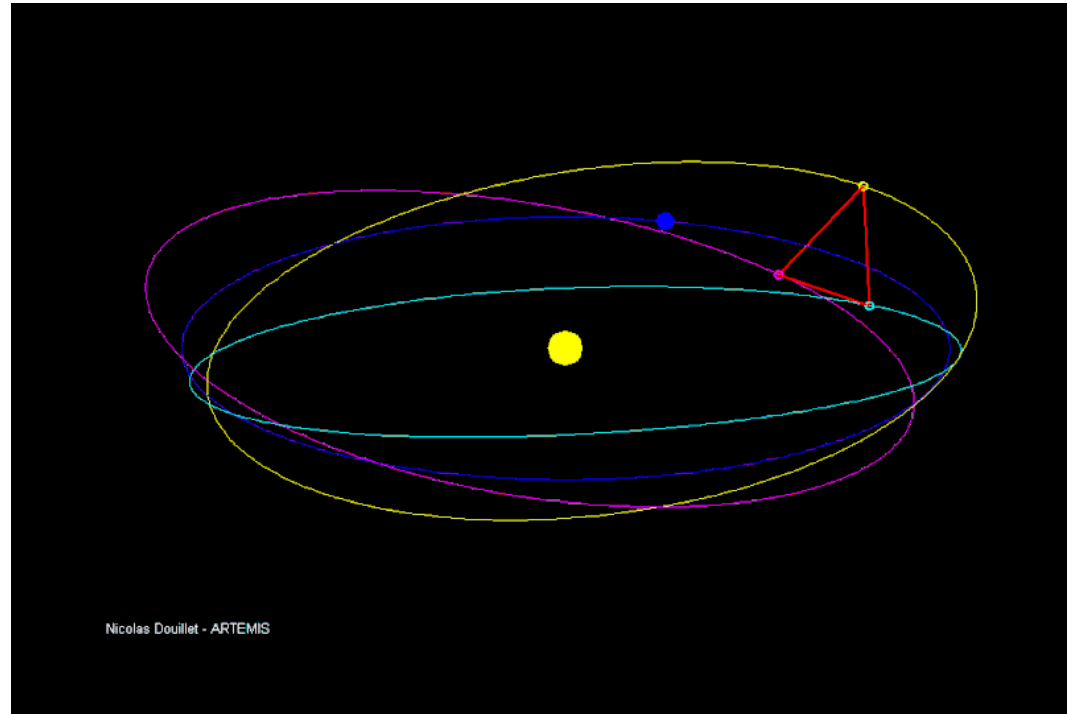
- LISA would be the first dedicated space-based GW detector using laser interferometry.
- The LISA concept has a constellation of three spacecraft arranged in an equilateral triangle with sides 2.5 million km long, flying along an Earth-like heliocentric orbit.
- The distance between the satellites is precisely monitored to detect a passing GW.
- The LISA project was initially as a joint effort between NASA and the ESA.
- LISA received its clearance goal for the 2030s, and was approved as one of the main research missions of ESA
- Each of the three LISA spacecraft contains two telescopes, two lasers and two masses (each a 2 kg cube of gold/platinum), arranged in two optical assemblies pointed at the other two spacecraft.



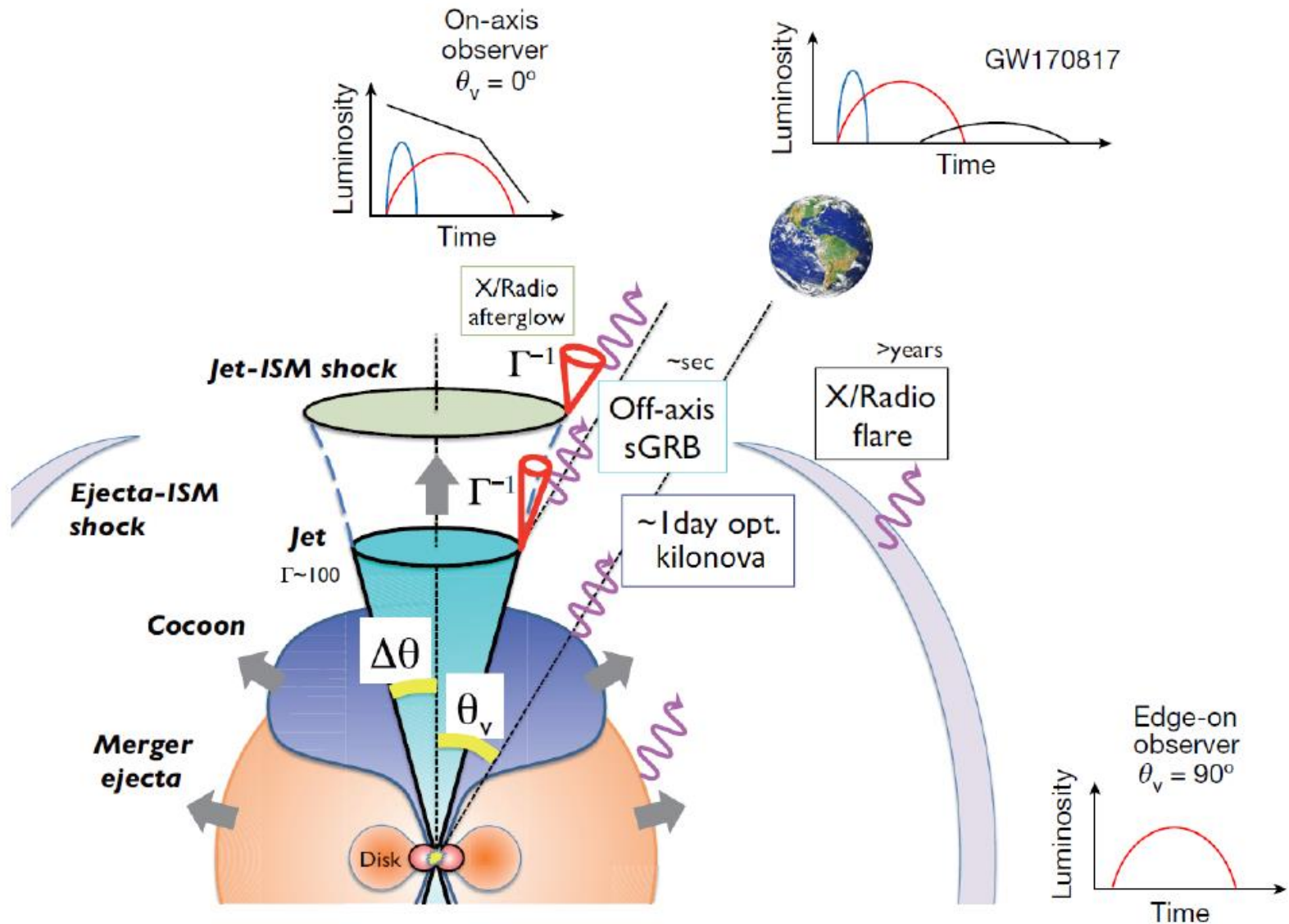
# The LISA interferometer in space

---

- The entire arrangement, 10xlarger than the orbit of the Moon, will be placed in solar orbit at the same distance from the Sun as the Earth.
- The approved 2017 LISA proposal has arms 2.5 million km long.
- An ESA test called LISA Pathfinder was launched in 2015 to test the technology necessary to put a test mass in (almost) perfect free fall conditions
- A LISA-like detector is sensitive to the GW low-frequency band, which contains many interesting sources




# The jet axis, X-ray, radio and neutrinos





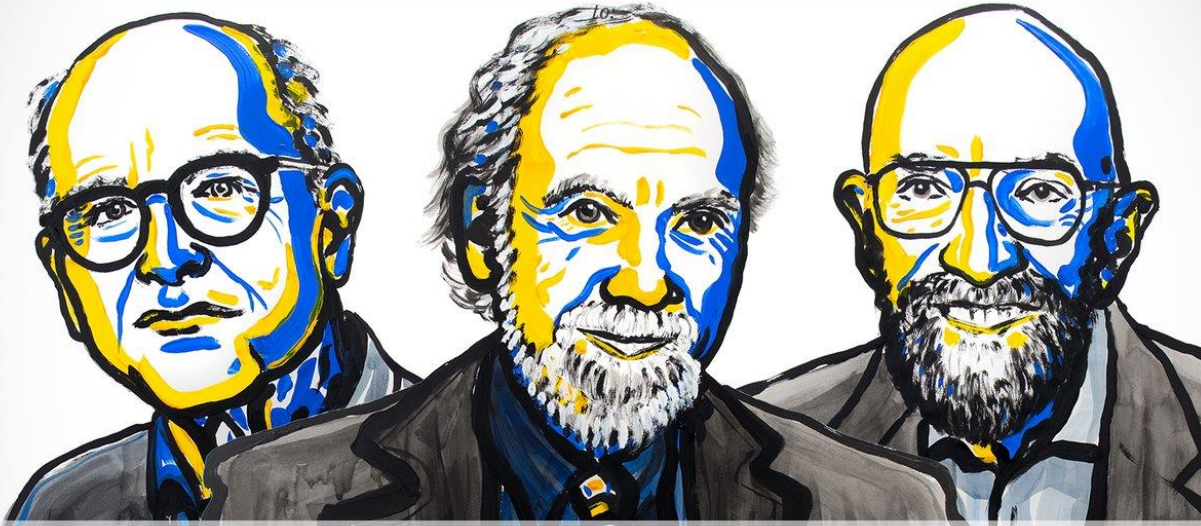
...for decisive contributions to the LIGO detector and the observation of gravitational waves

*"For the greatest benefit to mankind"*  
*Alfred Nobel*



The Royal Swedish Academy of Sciences has decided to award the

# 2017 NOBEL PRIZE IN PHYSICS



Illustrations: Niklas Elmehed, Nobel Prize Medal: © The Nobel Foundation, Photo: Lovisa Engblom.

## Rainer Weiss Barry C. Barish Kip S. Thorne

*"for decisive contributions to the LIGO detector and the observation of gravitational waves"*

M. Spurio - Astroparticle Physics - 13  
Nobelprize.org



# Due laureati della nostra Università



# Conclusions

---

- GWs exist and carry energy as expected after 60 y of debate
- GWs allow to investigate general relativity in a previously inaccessible regime.
- GW170817 represents the 1<sup>st</sup> event for which both GW and EM from a single astrophysical source have been observed, opening new perspectives also in fields different from astrophysics;
- They travel at the speed of light, in a Lorentz-invariant way
- GWs allows exploring the non-thermal Universe in a way completely independent by the electromagnetic radiation.
- Astrophysics of stellar-size BHs
- Cosmology: an independent “ladder” scale
- Measurement of the Hubble constant
- ....
- New LIGO/Virgo run O3: From April 2019.